

UNIVERSITY OF OKLAHOMA

GRADUATE COLLEGE

**CYTOSOLIC DELIVERY OF MUTANT FORMS OF TOXIN B FROM
CLOSTRIDIUM DIFFICILE FACILITATES CHARACTERIZATION OF THE
INTRACELLULAR ACTIVITIES OF LARGE CLOSTRIDIAL TOXINS**

A Dissertation

SUBMITTED TO THE GRADUATE FACULTY

In partial fulfillment of the requirements for the

degree of

Doctor of Philosophy

By

Lea Michelle Spyres

Norman, Oklahoma

2002

UMI Number: 3420666

All rights reserved

INFORMATION TO ALL USERS

The quality of this reproduction is dependent upon the quality of the copy submitted.

In the unlikely event that the author did not send a complete manuscript and there are missing pages, these will be noted. Also, if material had to be removed, a note will indicate the deletion.



UMI 3420666

Copyright 2010 by ProQuest LLC.

All rights reserved. This edition of the work is protected against unauthorized copying under Title 17, United States Code.



ProQuest LLC
789 East Eisenhower Parkway
P.O. Box 1346
Ann Arbor, MI 48106-1346

c Copyright by LEA MICHELLE SPYRES 2002

All Rights Reserved

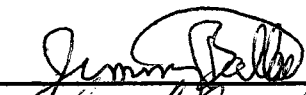
**CYTOSOLIC DELIVERY OF MUTANT FORMS OF TOXIN B FROM
CLOSTRIDIUM DIFFICILE FACILITATES CHARACTERIZATION OF THE
INTRACELLULAR ACTIVITIES OF LARGE CLOSTRIDIAL TOXINS**

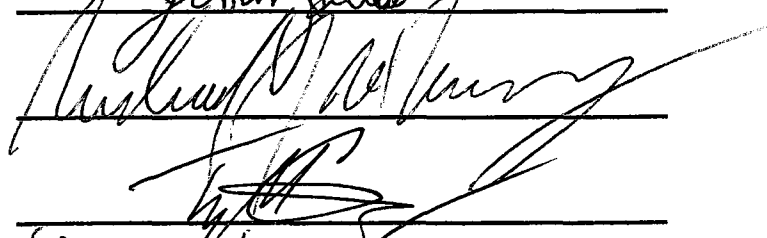
A Dissertation

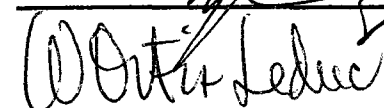
APPROVED FOR THE

DEPARTMENT OF BOTANY AND MICROBIOLOGY

BY









ACKNOWLEDGEMENTS

First of all, I would like to thank God and my family. This was an accomplishment that I could not have achieved on my own.

Secondly, I would like to thank my advisor for providing me with a great project and continuous support. I appreciate him making himself available to students at all times and I have enjoyed many stimulating scientific discussions. He never has a negative thing to say about anyone and works tirelessly in pursuit of scientific excellence. I could not have asked for a better graduate student advisor.

I appreciate the hard work and dedication of Amy Hensley and Jeremy Daniel on this project. I also appreciate the contribution of my long time lab members Maen Qa'Dan and Amy Meader. I would like to especially thank Mahdiah Parizi for late night conversations and coffee breaks in the lab. I would also like to say thank you to the more recent members of the Ballard lab: Lisa Dillon, Isabelle Salles, Dan Voth and Joy Wall, thanks for putting up with me and best of luck to you all.

Finally, I would like to thank my committee for their time spent and for important advise during the course of my graduate degree. I would especially like to thank Dr. Ortiz-Leduc, who I have had the privilege of working with over the past year. The Department of Botany and Microbiology has provided support in numerous ways. I would like to thank Gail, Beverly and Adell for their efforts. Many people have contributed to my success here at OU. If I have left anyone out please accept my heartfelt apology.

TABLE OF CONTENTS

ABSTRACT.....	viii
Literature Review.....	1
LCTs	2
The Ras superfamily of proteins.....	3
Ras proteins in human disease	4
The Rho family of Ras-related GTPases	5
Effectors of Rho proteins.....	9
Rho Proteins and Transcription	11
The Ras superfamily: Targets of bacterial toxins	14
LCTs- Structural Features.....	14
Anthrax Toxin Delivery System.....	18
LFnTcdB Fusion Proteins.....	18
MATERIALS AND METHODS.....	20
Tissue Culture, Mice, bacterial strains and chemical reagents.....	20
Bafilomycin A1 inhibition experiments	20
Cloning TcdB ₁₋₅₅₆ , TcdB ₁₋₅₀₀ , TcdB ₁₋₄₂₀ , TcdB ₁₋₁₇₀ , TcdB ₃₅₋₅₅₆ , and TcdB ₆₇₋₅₅₆	21
Site directed mutants.....	23
Expression and isolation of recombinant RhoA, Rac1, and Cdc42 substrates and PA	23
Isolation of LFnTcdB Fusion Proteins.....	25
Glucosylation assay	27
Cytotoxicity assay and mouse lethality	28
Actin Cytoskeleton Staining.....	29
Hydrolase assays.....	29
Inhibitor assays	31
Protection of CHO cells expressing LFnTcdB ¹⁻⁵⁵⁶	32
In vitro Inhibition experiments	33
Differential glucosylation of HeLa extracts from cells cotreated with LFnTcdB ¹⁻⁵⁰⁰ and TcdB.....	33
V8 protease digestion.....	34
RESULTS	35
Time Course of cytosolic entry for TcdB and TcsL	35
Purification of the TcdB enzymatic domain fused to LFn (LFnTcdB ¹⁻⁵⁵⁶).....	35
Analysis of the enzymatic activity of LFnTcdB ¹⁻⁵⁵⁶	43
The TcdB Glucosylation Domain Confers Lethality.....	47
Construction, Purification, and Characterization of Carboxy-terminal Deletions of LFnTcdB ₁₋₅₅₆	51
Inhibition of CPE from <i>C. difficile</i> supernatant.....	55
Inhibition of <i>C. sordellii</i> TcsL	57
Inhibition Inside the Mammalian Cell	57

In vitro Inhibition of TcdB.....	60
In vitro glucosylation of substrates prepared from cells treated with TcdB and inhibitor	60
Time-course of inhibition	60
Construction, Purification and Analysis of Amino-terminal Deletions and site-Directed Mutants of the TcdB Enzymatic Domain Fused to LFn.....	63
Hydrolase Activity of Site-directed Mutants of the TcdB Enzymatic Domain.....	66
V8 Protease Digestion	66
Differential Glucosylation	69
In Vivo Inhibition of TcdB.....	73
DISCUSSION	75

LIST OF FIGURES AND TABLES

Figure 1. Dendrogram of Rho family GTPases.	6
Figure 2. Sequence Alignments for RhoA, Rac1, and Cdc42.	7
Figure 3. RhoA Interaction With Regulatory Proteins.	10
Figure 4. RhoA Effector Proteins.	12
Figure 5. Rac and Cdc42 Effector Proteins.	13
Figure 6. Signaling Cascades Activated by Rho GTPases.	15
Figure 7. Chimeric Fusion Proteins.	17
Figure 8. Bafilomycin A1 Inhibition of TcdB Cytosolic Entry.	36
Figure 9. Bafilomycin A1 inhibition of TcsL Cytosolic Entry.	37
Figure 10. Nickel Column Purification of LFnTcdB ¹⁻⁵⁵⁶ and LFn.	38
Figure 11. Immunoblots of Purified LFnTcdB ¹⁻⁵⁵⁶ Expressed at 37°C and 16°C.	40
Figure 12. Immunoblots of Purified LFnTcdB ¹⁻⁵⁵⁶ Expression in different strains of <i>E. coli</i>	42
Figure 13. Glucosylation activity of TcdB and LFnTcdB ¹⁻⁵⁵⁶	45
Figure 14. Time-Course of CPE for TcdB and LFnTcdB ¹⁻⁵⁵⁶ plus PA.	46
Figure 15. Dose Curve Response of TcdB and LFnTcdB ¹⁻⁵⁵⁶ plus PA CPE.	48
Figure 16. Actin Staining.	49
Figure 17. Glucosylation of Recombinant Substrates RhoA, Rac1, and Cdc42.	52
Figure 18. Delayed CPE of TcdB.	53
Figure 19. Inhibition of TcdB CPE by the continued addition of LFnTcdB ¹⁻⁵⁰⁰	54
Figure 20. Inhibition of CPE from a <i>C. difficile</i> supernatant.	56
Figure 21. LFnTcdB ¹⁻⁵⁰⁰ Inhibition of TcsL CPE.	58
Figure 22. Inhibition of CPE in CHO Cells Expressing the Enzymatic Domain of TcdB.	59
Figure 23. In vitro Competition.	61
Figure 24. Differential Glucosylation of Extracts Treated With TcdB or TcdB Plus Inhibitor.	62
Figure 25. Inhibition of TcdB CPE prior to or following TcdB Treatment.	64
Figure 26. Glucosylation and CPE of LFnTcdB Site-Directed Mutants.	67
Figure 27. V8 Protease digestions of LfnTcdB Site-Directed Mutants.	70
Figure 28. Summary of LFnTcdB Deletion Mutants and Site-Directed Mutants.	71
Figure 29. Differential Glucosylation.	72
Figure 30. Inhibition of TcdB by LFnTcdB Amino-Terminal Deletion Mutants and Site-Directed Mutants.	74
Figure 31. Model for TcdB and TcsL Inhibition.	83
Table 1. Primers for Generation of TcdB Deletion Mutants.	22
Table 2. Primers for Generation of Site-directed Mutants.	24
Table 3. Hydrolase Activity of LFnTcdB ¹⁻⁵⁵⁶	41
Table 4. Lethal Effects of LFnTcdB ¹⁻⁵⁵⁶	47
Table 5. Glucosylhydrolase activity of LFnTcdB Mutants.	67

ABSTRACT

Clostridia are gram-positive spore-forming organisms responsible for a variety of diseases in both humans and animals. Three species of Clostridia- *Clostridium difficile*, *Clostridium sordellii* and *Clostridium novyi*- produce a unique class of toxins termed large clostridial toxins (LCTs). These toxins inactivate members of the Ras superfamily of mammalian GTPases by glycosylation. LCTs are important in a variety of diseases, for example, Toxin A (TcdA) and toxin B (TcdB) are the major virulence factors in *C. difficile* associated diarrhea and pseudomembranous colitis. Whereas *Clostridium sordellii* lethal toxin (TcsL) and *Clostridium novyi* alpha toxin (Tcn α) have been implicated in gas gangrene infections. In addition to their roles in disease, TcdB and TcsL have been extensively used to decipher the effects of inactivating Ras proteins in mammalian cells. In order to better understand the role of these toxins in inactivating Ras proteins, we have undertaken the molecular characterization of intoxication by two LCTs, TcsL and TcdB. A chimeric fusion protein consisting of the TcdB enzymatic domain fused to the binding and translocation regions of anthrax lethal toxin (LFnTcdB¹⁻⁵⁵⁶) was able to confer cytopathic effects on tissue culture cells and in a mouse, when delivered with the protective antigen (PA) component of anthrax toxin. Fusions containing mutants in the enzymatic domain of TcdB (LFnTcdB¹⁻⁵⁰⁰, LFnTcdB¹⁻⁴²⁰, LFnTcdB¹⁻¹⁷⁰, LFnTcdB³⁵⁻⁵⁵⁶, LFnTcdB⁶⁷⁻⁵⁵⁶, LFnTcdB^{C365S}, LFnTcdB^{C365W}, LFnTcdB^{W102A}) were inactive for glucosylation and CPE on cells, with the exception of LFnTcdB^{C365S} and LFnTcdB¹⁻¹⁷⁰. The fusion proteins attenuated in enzymatic activity acted as inhibitors of TcdB both in vivo and in vitro. LFnTcdB1-500 was also able to

inhibit the activity of TcsL and slowed cell rounding in transformed mammalian cells expressing the enzymatic domain of TcdB indicating the competition was occurring inside the cytosol. A combination of the lysosomotropic agent Bafilomycin A1 and the LFnTcdB1-500 inhibitor was used to determine the time required for cytosolic entry and irreversible cytopathic effects after treatment with TcdB. Furthermore, the time required for TcsL cytosolic entry was found to be considerably slower than that of TcdB accounting for the lower CPE of TcsL compared to TcdB.

Literature Review

A variety of bacteria secrete extracellular toxins capable of entering into and modifying mammalian cells. The most frequent means of accomplishing cellular entry appears to be via receptor mediated endocytosis. After being internalized, the toxin must traffic to the cytosol where it carries out its enzymatic action. To this effect, the toxin or at least an active fragment of the toxin, must translocate from the lumen of the endocytic vesicle into the cytosol. Endosomal acidification may be required for insertion and translocation across the vesicular membrane. In addition, many toxins including anthrax toxin, ricin, diphtheria toxin, and *Pseudomonas* exotoxin require proteolytic cleavage and/or reduction for activation [1]. Unfortunately, the mechanisms of entry and intoxication for LCTs have not been well studied.

The mechanism of action of LCTs is of particular interest since *Clostridium sordellii* and *Clostridium novyi* toxins have been implicated in gas gangrene infections and *Clostridium difficile* TcdA and TcdB are major virulence factors in *C. difficile* associated disease (CDAD) [2]. An estimated 300,000-3,000,000 people in the United States contract CDAD each year [2]. While CDAD is usually mild, the disease can be quite severe and 15-30 percent of those affected relapse within 2 months after treatment [3]. CDAD can be fatal in the elderly and immune suppressed, and *C. difficile* infections have become an increasing problem for individuals suffering from AIDS [4].

TcdA acts as an enterotoxin and is considered to be the major cause of fluid accumulation and diarrhea caused by *C. difficile*; while, TcdB is an effective cytotoxin, possesses 1000 times greater enzymatic activity than TcdA, and is responsible for systemic intoxication [5]. The role of *C. sordellii* and *C. novyi* LCTs in wound infections is not as well understood. Due to the large size of LCTs and the lack of genetic techniques for manipulating clostridia, these toxins have not been extensively characterized. Gaining a basic understanding of the structure/function of these toxins may lead to improved therapies for clostridial infections involving LCTs.

LCTs

The LCTs are a unique class of virulence factors generated by at least three pathogenic clostridial species. *C. difficile* produces TcdA and TcdB, *C. novyi* makes Tcn α , and *C. sordellii* produces TcsL and hemorrhagic toxin (TcsH). These toxins are exceptionally large (ranging from 260-308 kDa) and function as glycosyltransferases to inactivate Ras proteins [5-7]. TcdA, TcdB, TcsL, and TcsH all use UDP-glucose as a cosubstrate, whereas alpha-toxin uses UDP-N-acetyl glucosamine to modify target substrates.

Since LCTs disrupt GTPase coordinated activities, they have proven to be valuable molecular tools for dissecting the roles of Ras proteins in cellular physiology. *C. difficile* TcdB is a LCT that modifies Rho proteins by glucosylation at T35 of Rac and Cdc42 (T37 for RhoA) resulting in the inactivation of downstream signaling pathways. TcdB, disrupts tight junctions, increases epithelial permeability, and promotes actin

condensation and cell death [8-10]. TcsL, on the other hand, modifies Ras, Rac, and Rap [11]. More recently TcsL has also been shown to target Ral and Cdc42 and to a much lesser extent RhoA [12]. Ras proteins control growth and differentiation, and glucosylation of Ras proteins at T35 by TcsL also results in inactivation and cell death.

The Ras superfamily of proteins

The first of the Ras proteins were discovered in the 1970s using animal tumor virus models; however, they were of little interest until 1982 when the gene encoding H-ras became the first identified human oncogene [13]. Since then, a widespread interest in Ras proteins has led to the identification of over 80 Ras related proteins, all of which are categorized under the Ras superfamily. The Ras superfamily of proteins share at least 30% homology and are further divided, based on sequence and functional similarities, into 5 families: Ras, Rho, Rab, Arf and Ran. These proteins act as molecular switches by cycling between an inactive GDP bound and an active GTP bound form. Ras proteins receive intracellular and extracellular (mediated through integral membrane proteins) signals and transmit these signals by activating specific kinase cascades. These kinase cascades result in the coordinated control of a variety of cellular functions including endocytosis, secretion, transcription, protein modification, cell migration, actin cytoskeleton dynamics and cell cycle progression, which collectively regulate cell growth (for reviews see[14, 15]).

Ras proteins in human disease

Since the discovery of Ras in tumor transformation there has been an intense interest in the function of these small GTP binding proteins. Mutations in Ras have now been identified in over 30% of lung adenocarcinoma and myeloid leukemia. While Ras mutations occur as often as 50% and 90% in colon adenocarcinoma and pancreas adenocarcinoma, respectively [16]. Although constitutively active Rho GTPases do not lead to cell transformation, these proteins play a role in metastasis, invasion and angiogenesis [17, 18]. Several Rho activating proteins are known oncogenes and apparently transform cells in a Ras independent manner. In addition to their role in cancer, the Ras superfamily of proteins have been linked to several physiological functions including embryo development, bone formation, neuronal growth, neurotransmitter exocytosis, muscle contraction, endothelial cell migration associated with wound repair, and migration of immune system cells in inflammatory response [19-21]. Not surprisingly, these proteins are now being linked to genetic disorders (Faciogenital dysplasia), immune system disorders (Human phagocyte immunodeficiency), and vesicular disorders (hypertension, cerebral vasospasm, myocardial hypertrophy) [22-24]. Ras proteins control a plethora of cellular and physiological functions and although it is beyond the scope of this dissertation research, are potential drug targets for a variety of diseases.

The Rho family of Ras-related GTPases

The Rho family of Ras related GTPases is composed of 10 different members (some with multiple isoforms) as diagrammed in Figure 1 [14]. RhoA, Rac1, and Cdc42 are the best understood of the Rho family GTPases, and are targets for *C. difficile* TcdB *in vitro* [25]. While isoforms of RhoA, Rac1, and Cdc42 have not been determined to be substrates for glucosylation, the similarity of the Rho proteins suggest they are all targets for modification by TcdB.

Rho proteins share many common structural features and possess intrinsic GTPase activity. Modifications in regions conferring the GTPase activity produce constitutively active GTP bound forms, while modifications that prevent the exchange of GDP for GTP result in inactivation of downstream signaling (Figure 2). The crystal structures of Rho, in both the GDP and GTP bound forms, reveal that the exchange of GDP for GTP causes structural changes in loop 1 (26aa-45aa) and loop 2 (59aa-74aa) exposing recognition sites for effector proteins [26, 27]. An insert region (123aa-135aa) is the major distinguishing characteristic of Rho family GTPases that differentiates them from other members of the Ras family, and in the case of Rac, this region is also involved in effector binding [28]. The Rho family of GTPases is highly conserved in amino acid composition as well as in function, and the major effects of sequence variations seem to be on their ability to interact with specific regulatory and effector proteins.

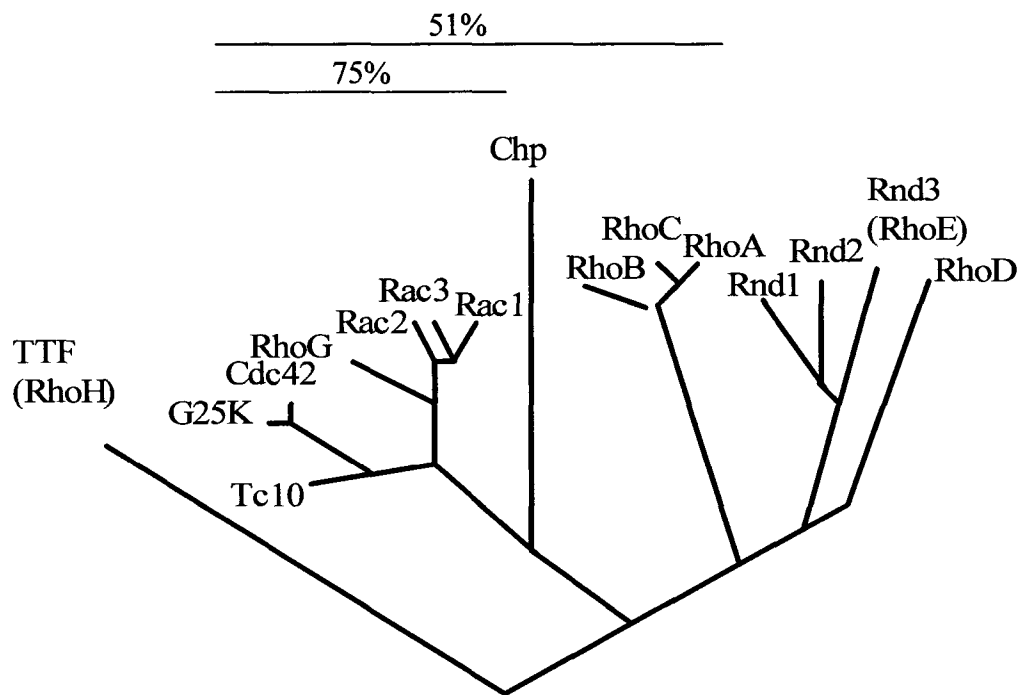


Figure 1. Dendrogram of Rho GTPases. This dendrogram shows the relative homology, at the amino acid level, of the Rho family members. Differential splicing results in multiple isoforms for Rnd, Rho, and Rac proteins. Additionally, G25K is an isoform of Cdc42. Rho, Rac and Cdc42 share 51% homology overall, while Rac and Cdc42 are 75% homologous.

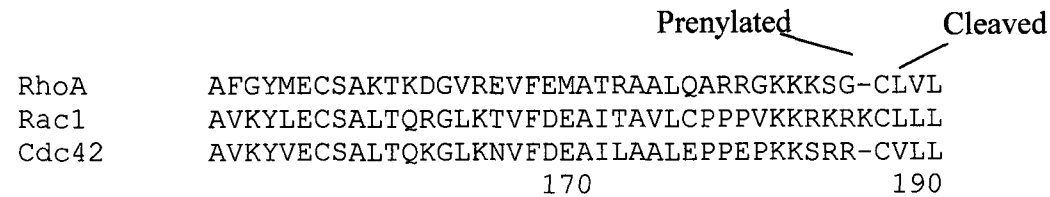
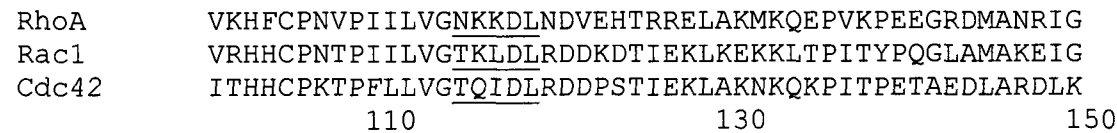
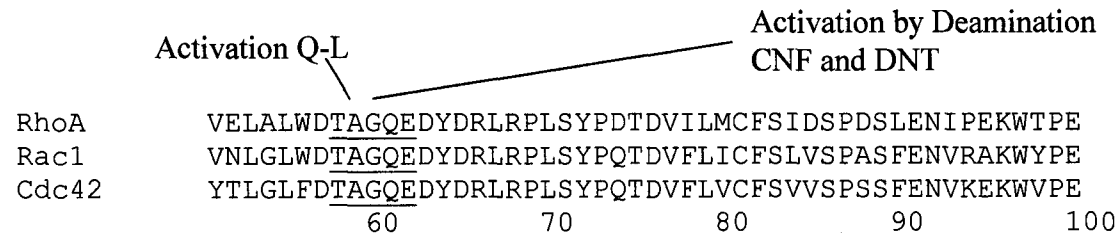
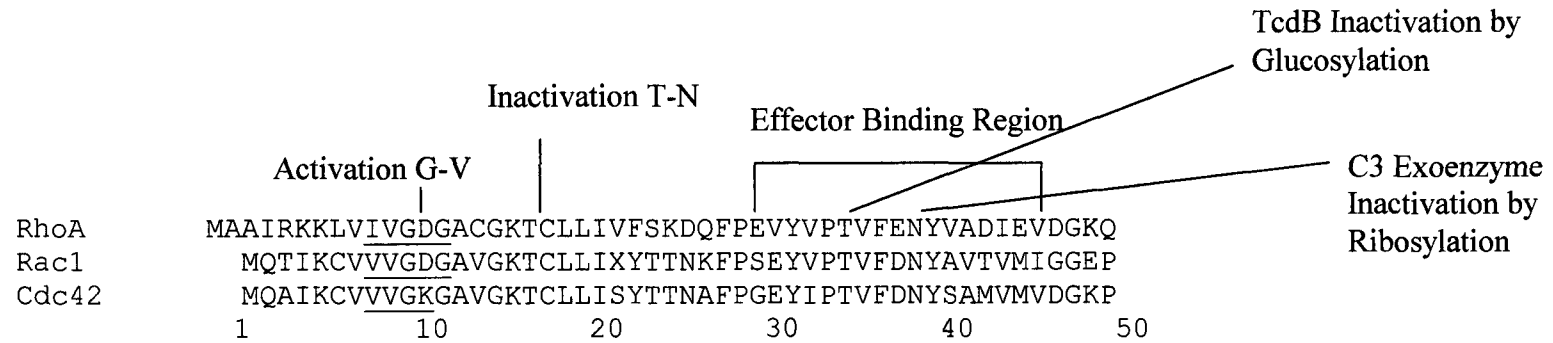


Figure 2. Sequence Alignments for RhoA, Rac1, and Cdc42. The effector-binding region of RhoA, Rac1, and Cdc42, indicated in the figure, interacts with downstream effector proteins and is also the site of modification by TcdB and C3 exoenzyme from *Clostridium botulinum*. Sequences indicative of GTPase activity are underlined and mutations in at least two of these regions result in constitutively active GTP bound forms of the proteins. Cytotoxic Necrotizing Factor (CNF) and Dermonecrotic Toxin (DNT) from *E. coli* also produce constitutively active forms of the GTPases by deaminating Q61. The site for cleavage and isoprenylation (required for recruitment to the membrane where they carry out their activity) is indicated in this figure as well.

The activation state of Rho proteins depends on the interaction of Rho with one of three regulatory proteins. Two regulatory factors are responsible for maintaining Rho in an inactive GDP bound form: GTPase activating protein (GAP) and Guanine dissociation Inhibitor (GDI). These regulatory proteins stimulate intrinsic GTP hydrolysis and stabilize the GDP bound cytosolic form of Rho proteins, respectively. Guanine exchange factors (GEFs) are the central regulatory factor in Rho activation, they respond to a variety of cellular signals and activate Rho by catalyzing the exchange of GDP for GTP.

The interaction between Rho and its regulatory proteins is complex. For instance, RhoA alone associates with at least 7 different GAPs and GEFs (Figure 3). In addition, 5 of the RhoA GEFs and 5 of the GAPs are shared with at least one other Rho family member. Recent experiments suggest that in addition to responding to activation signals, GEFs may also regulate the affinity of Rho proteins for specific effector proteins, at least for Rac and Cdc42 [29]. GEFs, GAPs, and GDIs act on Rho proteins controlling the activation state and effector interaction of Rho family proteins.

Effectors of Rho proteins

Each GTPase binds to specific effectors and activates phosphorylation cascades. The GTP bound form of RhoA interacts with several effectors, which are divided into three groups according to homology in the RhoA binding region. The regions are called Rho effector motif class 1 (REM), ROK kinectin homology region class 2 (RKH), and a third class of effectors that do not share homology with either the REM or the RKH domains.

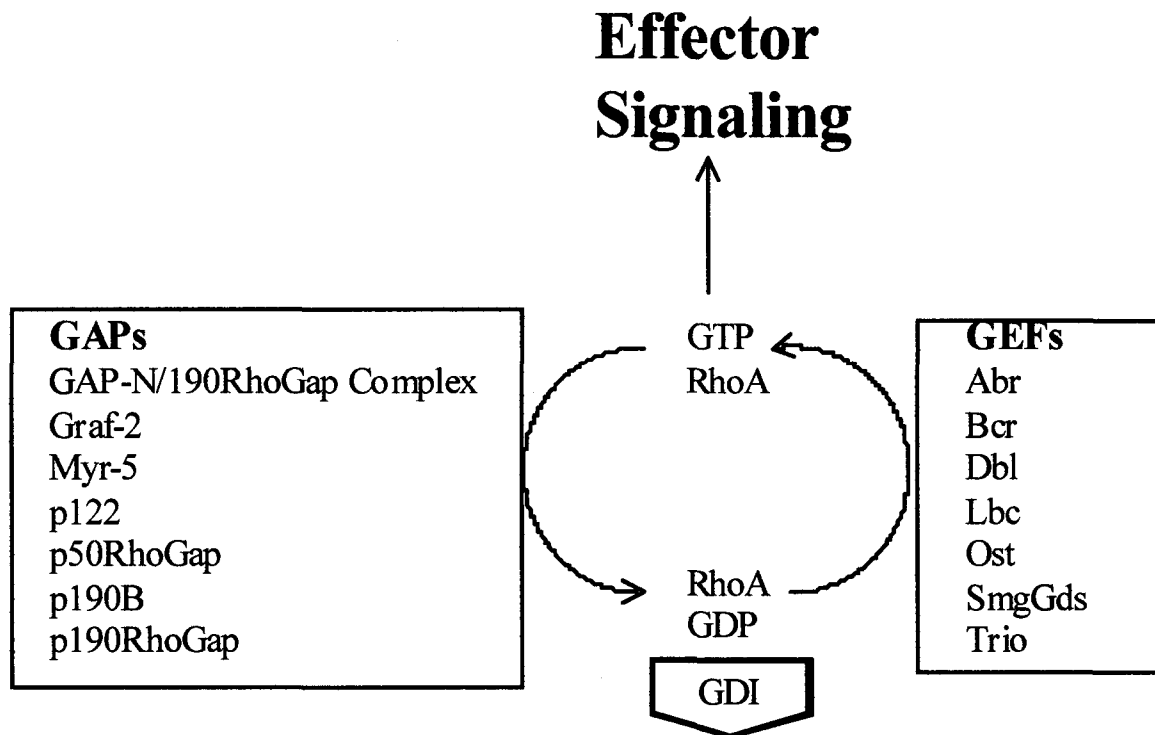


Figure 3. RhoA Interaction With Regulatory Proteins. Multiple GAPs interact with RhoA and stimulate GTP hydrolysis. GDI maintains the inactive (GDP bound) form of RhoA in the cytosol and GEFs (of which there are also multiple forms) stimulate the exchange of GDP for GTP allowing the protein to cycle from the cytosol to the membrane and activate downstream effector proteins.

A complete list of RhoA effectors can be seen in Figure 4. Rac and Cdc42 are more closely related to each other than to RhoA, and share many of the same effector proteins (Figure 5). Several of the Rac and Cdc42 targets share a common Rac/Cdc42 binding motif (CRIB). RhoA shares 5 effector proteins with Rac and has no common effectors with Cdc42 (for a review see [30]). The effectors of the other Rho family members have not been identified.

Rho Proteins and Transcription

Several of the signaling pathways for Rac and Cdc42 effector kinases have been deciphered. For example, JNK a common Rac and Cdc42 target protein activates a signaling cascade that results in the activation of c-Jun and c-Fos transcription factors, which activate transcription at the AP1 promoter element. Additionally, p38K may also be activated downstream of PAK, activating the ATF transcription factor and initiating transcription at the cyclic AMP response element (CRE) [31, 32]. Rho has been recently shown to induce expression from the serum response element (SRE) through transcriptional activation of serum response factor (SRF) (see Figure 6) [33]. Generally these cascades are very specific, however some cross talk occurs between pathways. Adding to the complexity, in some cases, it may be necessary for these transcription factors to form complexes with other protein factors before initiating transcription at certain promoters. Bacterial toxins that activate or inactivate Ras related GTPases are ideally suited to study further these signal transduction pathways.

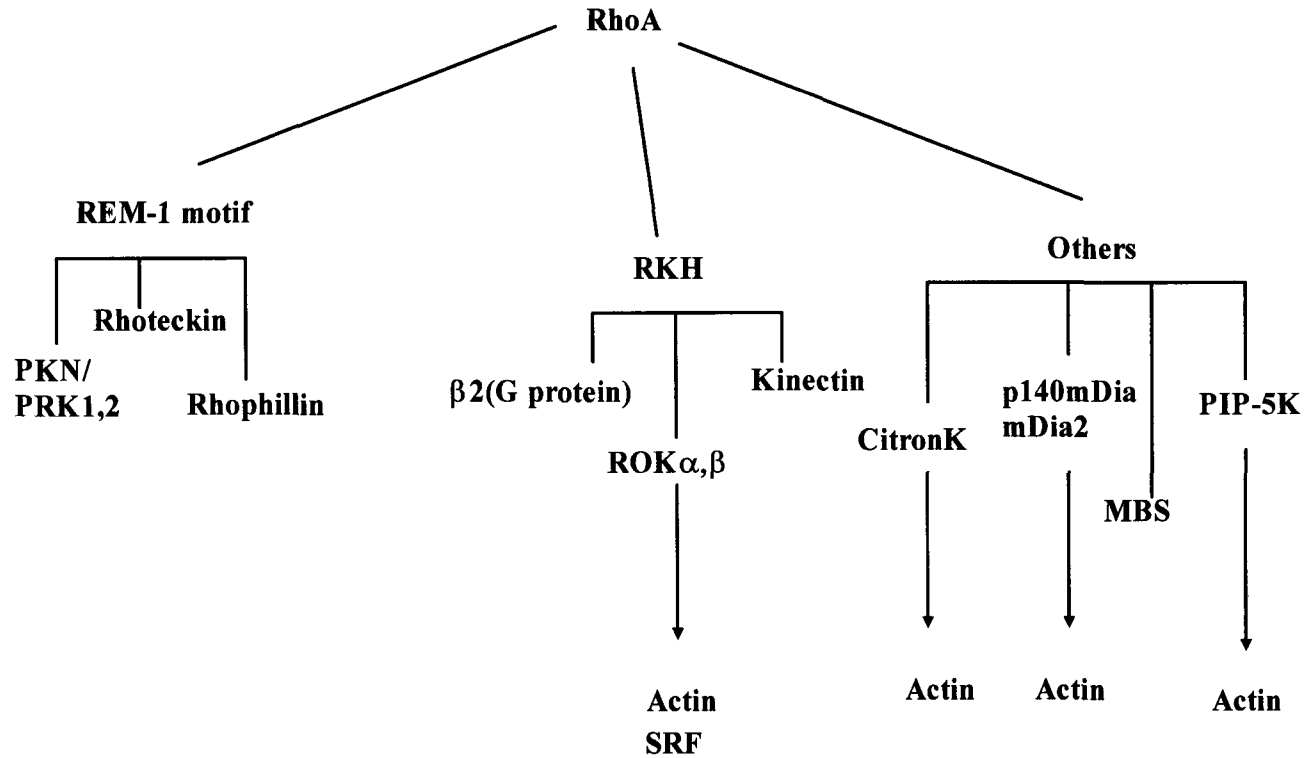


Figure 4. RhoA effector proteins. RhoA interacts with a variety of downstream effectors, which include kinases, structural proteins, and heteromeric G proteins. These effectors can be divided into three groups based on different RhoA binding regions: REM, RKH, and a third with no homology to the first two. Either directly or indirectly, these effectors regulate actin polymerization and organization.

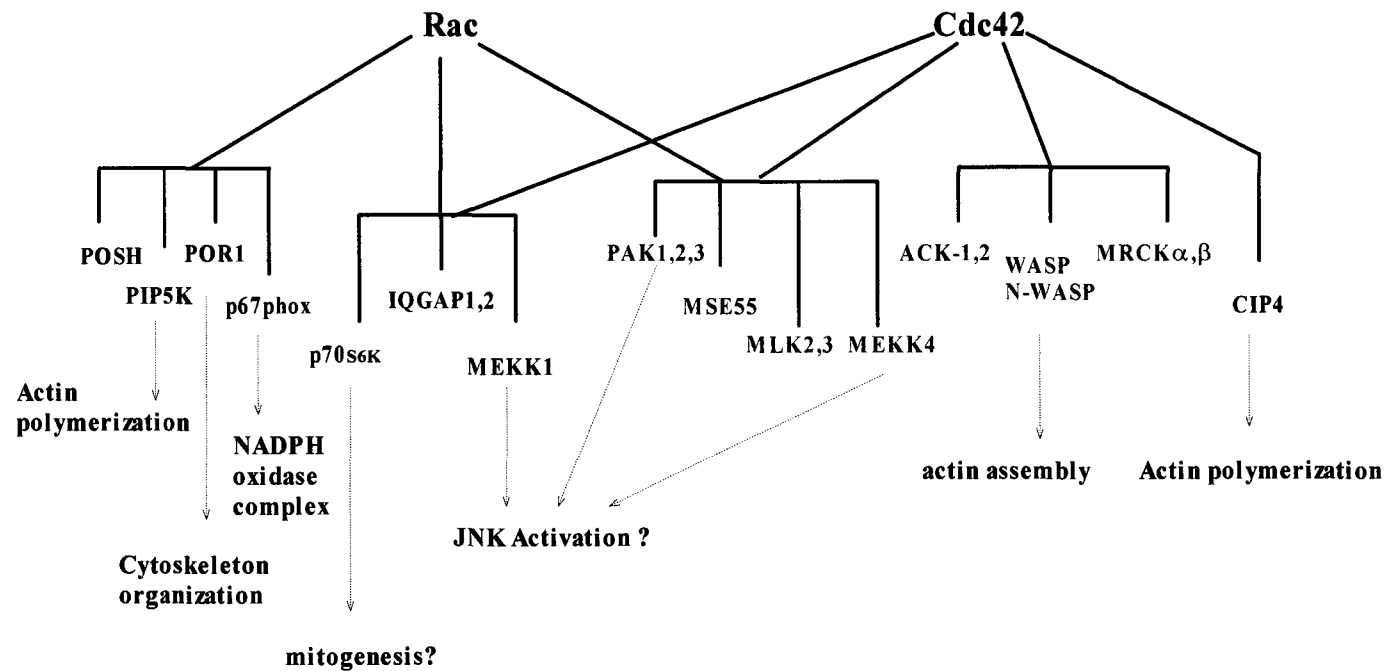


Figure 5. Downstream effector proteins for Rac and Cdc42. Rac activates effector proteins involved in the regulation of actin polymerization and cytoskeleton organization, as well as regulation of NADPH oxidase complex. Cdc42 also regulates actin assembly and polymerization through interaction with different effector proteins. Both Rac and Cdc42 activate Jun-N-terminal kinase and stimulate mitogenesis. The effectors that interact with the common Rac, Cdc42 CRIB binding motif are shown in red.

The Ras superfamily: Targets of bacterial toxins

In addition to being potential drug targets, Ras related GTPases are the most common intracellular targets of bacterial virulence factors. Protein toxins produced by gram-positive and gram-negative bacteria are responsible for both inactivating and activating Ras and/or Rho GTPases. For example, *Escherichia coli* cytotoxic necrotizing factor (CNF) and *Bordetella bronchiseptica* dermonecrotic toxin (DNT) deaminate Glu63 blocking GTPase activity and activating Rho by locking it in the GTP bound form [34]. Inactivating toxins include the 5 LCTs. Exoenzyme S produced by *Pseudomonas aeruginosa* activates Rho family members but inactivates Rab and Ras family GTPases [34, 35]. Clearly, the study of Ras superfamily proteins is far reaching since it impacts our understanding of numerous human pathogens.

LCTs- Structural Features

Like many intracellular toxins, LCTs can be roughly divided into enzymatic, translocation and receptor binding domains. The amino-terminal end of LCTs contain the enzymatic domain, followed by a hydrophobic region believed to be involved in translocation and then finally the receptor-binding domain located within the carboxy-terminal third of the toxin [34]. Through deletion studies, the enzymatic domain has been narrowed to approximately 550 amino acids [12, 36, 37]. Further deletions at the 3' end of this fragment have been shown to attenuate enzymatic activity and deletion of the first 244 residues renders TcdB enzymatically inactive [38]. Within the enzymatic region, tryptophan 102 has been shown to be involved in UDP-glucose binding for TcdB, TcsL,

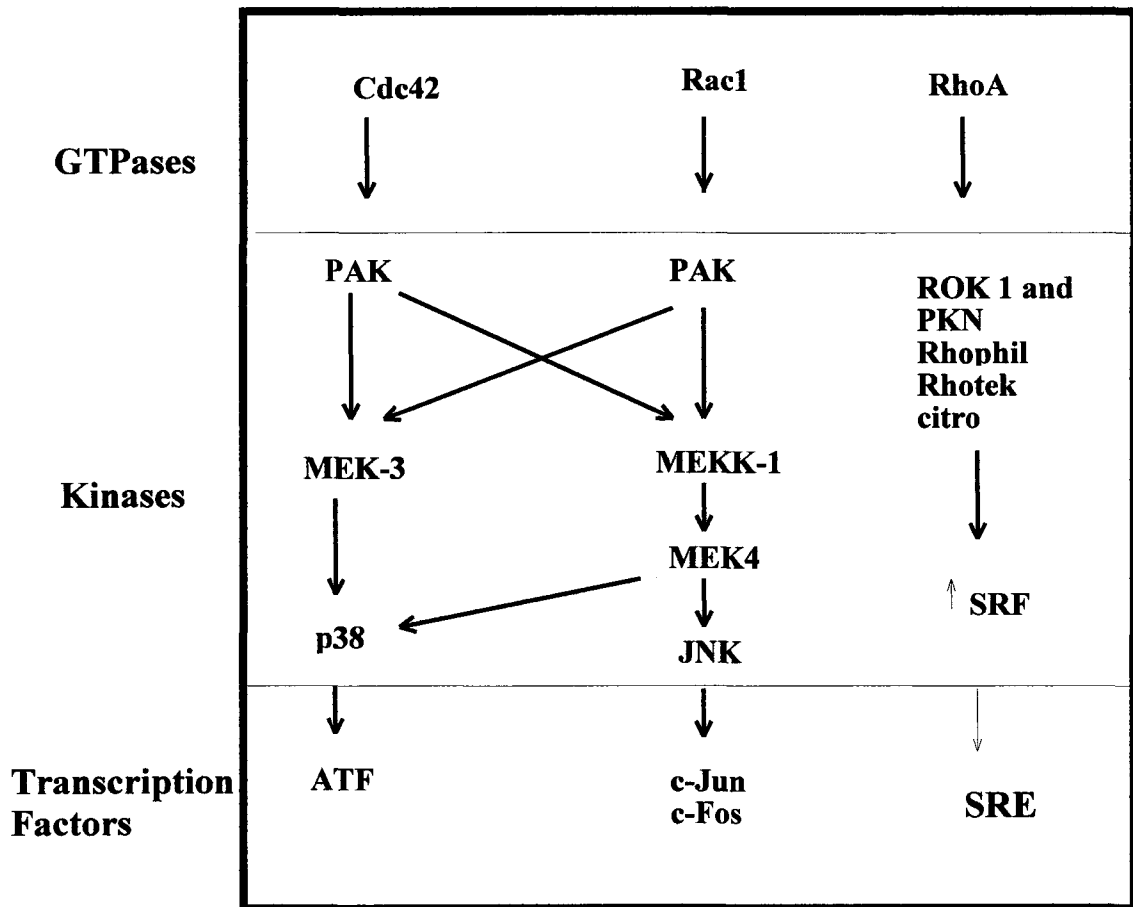


Figure 6. Signaling cascades activated by Rho GTPases. Rac and Cdc42 activate Protein Activating Kinase (PAK) leading to the activation of ATF, c-jun and c-fos transcription factors. Rho acts through one of several effector proteins to activate serum response factor (SRF) leading to activation of transcription at the serum response element.

and α -toxin [39]. Additionally, a DXD motif at position 286-288 which is common to a group of glucosyltransferases has been identified as important for glucosylhydrolase activity of LCTs [39]. The substrate recognition region has been narrowed to the carboxy-terminal region of the enzymatic domain, but the exact residues involved in substrate recognition have not been identified. Exchange of residues 364-468 of TcsL for those residues of TcdB change substrate targeting to favor TcdB target GTPases, while exchange of the same residues of TcdB for those of TcsL does not favor targeting of Ras, Rap, and Ral [12]. Smaller substitutions have not been tested for substrate recognition. Taken together these results indicate that the residues responsible for binding Rho, Rac, and Cdc42 are located somewhere between residues 364-468, while the Ras, Rap and Ral recognition residues lie somewhere between residues 364-516, see Figure 7 [12]. Truncated forms of TcdB have been expressed in *E. coli* and the enzymatic domain has been partially characterized using this approach, however, characterization of deletion mutants was precluded by lack of receptor binding/translocation functions and it was necessary for these mutants to be microinjected [36, 38]. Furthermore, the requirement for microinjection prevented analysis of the enzymatic domain in animal models. To address these problems we have utilized a translocation active, yet non-toxic, form of anthrax toxin to deliver the enzymatic domain of TcdB (TcdB¹⁻⁵⁵⁶) and mutant derivatives to the cytosol of mammalian cells.

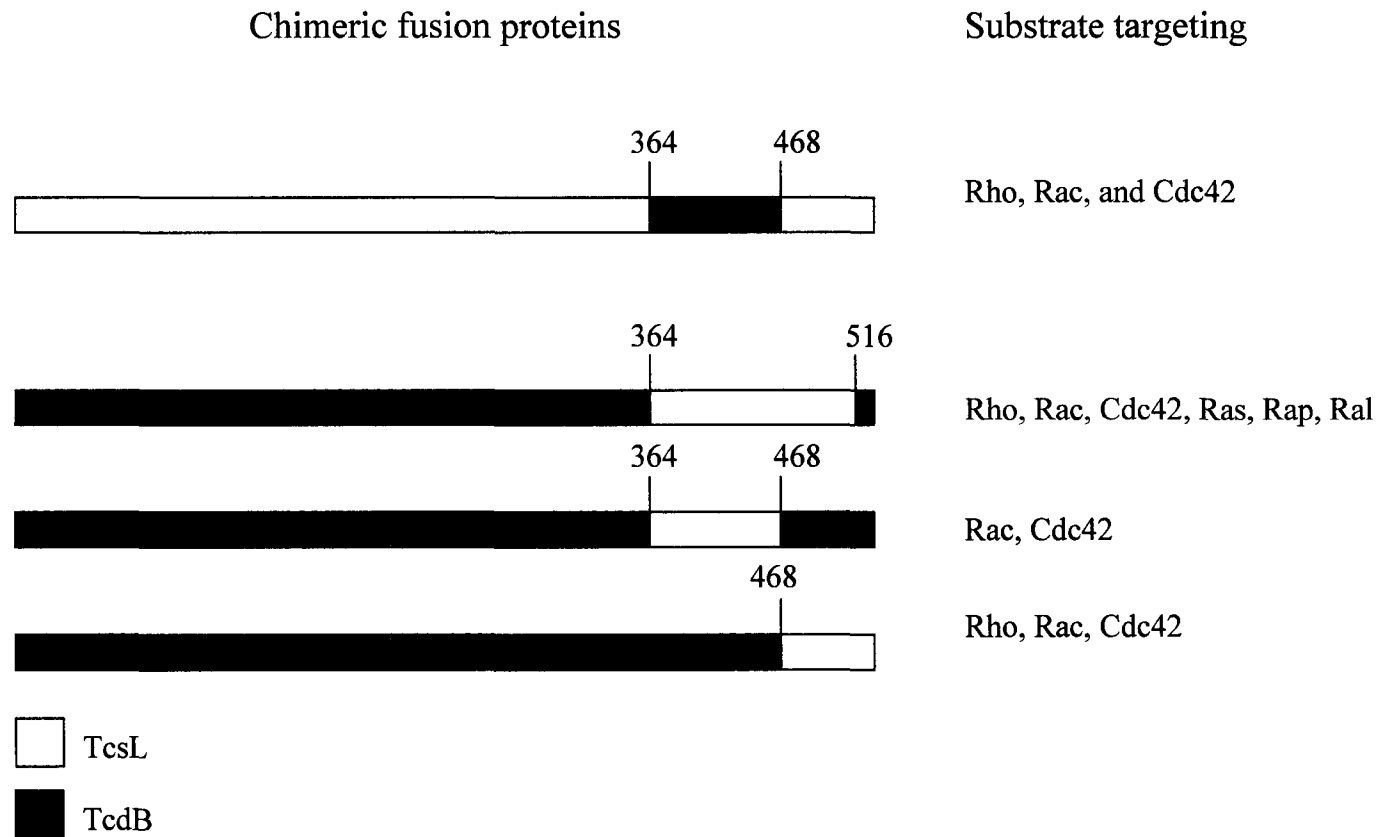


Figure 7. Chimeric fusions of the enzymatic domains of TcsL and TcdB. The substrate recognition region of TcdB was found to reside somewhere within residues 364-516. Recognition of TcsL substrates (Ras, Rap, and Ral) required both this region, and the region between 468-516.

Anthrax Toxin Delivery System

Anthrax toxin is a tripartite bacterial toxin in which protective antigen (PA) mediates the cytosolic delivery of lethal factor (LF) or edema factor (EF). Previous work by Arora et al. [40] and Milne et al. [41] showed that a translocated form of LF (LFn: 254 residues) could be used in conjunction with PA as a delivery system to carry heterologous polypeptides into the cytosol of mammalian cells. In subsequent work [42] the PA-LFn system has been used to deliver the enzymatic domains of intracellular toxins, as well as, a novel approach for priming cytotoxic T-lymphocyte [43, 44].

LFnTcdB Fusion Proteins

In this work, the enzymatic domain of TcdB fused to LFn (LFnTcdB¹⁻⁵⁵⁶) was delivered to cells and was found to confer similar effects as native TcdB in tissue culture cells and in a mouse model system [45]. Additionally, fusions of three carboxy-terminal deletions (LFnTcdB¹⁻⁵⁰⁰, LFnTcdB¹⁻⁴²⁰, LFnTcdB¹⁻¹⁷⁰), two amino terminal deletions (LFnTcdB³⁵⁻⁵⁵⁶, LFnTcdB⁶⁷⁻⁵⁵⁶) and three site directed mutants (LFn^{C395S}, LFn^{C395W}, LFn^{W102A}) were generated and tested for the ability to hydrolyze UDP-glucose and transfer the glucose moiety to Rho protein substrates. During the analysis of these fusion proteins, we discovered a set of mutant proteins unable to modify substrate were capable of blocking TcdB cytopathic effects. Herein I describe the generation and analysis of these mutants and detail the role of these proteins as inhibitors of LCTs. In addition to providing insight into the functional domain of TcdB, these mutants also suggest a new type of

therapeutic approach that could ameliorate the symptoms caused by intracellular virulence factors.

MATERIALS AND METHODS

Tissue Culture, Mice, bacterial strains and chemical reagents

Chinese Hamster Ovary-K1 (ATCC) cells were maintained in Ham's F-12 medium (Gibco BRL) supplemented with 10% fetal bovine serum. Human cervical adenocarcinoma cells ATCC CCL-2 (HeLa) were grown in supplemented RPMI 1640 (RP-10) [46] with 10% fetal bovine serum. Human Fetal Lung Fibroblasts (GM05387; NIGMS Human Genetic Mutant Cell Repository, Camden, NJ) between passage 8 and 21, were grown in complete medium (MEM with high glucose Gibco BRL) 200U/ml penicillin and 200µg/ml streptomycin). Tissue culture cells were incubated at 37°C in a humid atmosphere with 6% CO₂. All mice were female BALB/c (Jackson Laboratories), between 8 and 12 weeks of age. *Clostridium difficile* strain VPI 10463 and *Clostridium sordellii* strain 9714 were obtained from ATCC and used as a source of culture supernatant, genomic DNA, TcdB and TcsL. All reagents were of molecular biology grade and were purchased from Sigma Chemical Company unless otherwise noted.

Bafilomycin A1 inhibition experiments

A time course of TcdB cytosolic entry was performed in a 96 well plate. CHO cells (5×10^4 cells/well) were plated in a volume of 100 µl RP10 and allowed to adhere overnight. The following day, cells were treated with or 200 fmol TcdB. Bafilomycin A1 (5×10^{-7}

M) was added to TcdB treated wells at 10-minute intervals up to 80 min. CPE were determined by cell rounding and were recorded at 8 and 16 hours after initial toxin treatment. A similar experiment was performed using TcsL (1 pmol). For the TcsL experiment, Bafilomycin A1 was added at two additional time points (100 and 120 min) and CPE were recorded after 16 hours.

Cloning TcdB₁₋₅₅₆, TcdB₁₋₅₀₀, TcdB₁₋₄₂₀, TcdB₁₋₁₇₀, TcdB₃₅₋₅₅₆, and TcdB₆₇₋₅₅₆

Clostridium difficile genomic DNA was isolated using an Easy-DNA™ Kit (Invitrogen) according to the manufacturer's instructions. A 1665 nucleotide fragment was amplified from the 5' end of *tcdB*. *lfn* was genetically fused with *tcdB*₁₋₁₆₆₅ by cloning the fragment into the *Bam*HI site of pABII, a derivative of pET15b, which contains the *lfn* gene with a 3' multiple cloning site, to make the plasmid pLMS200. Using a similar approach, five other fusions of LFnTcdB were also constructed. Briefly, fragments encoding regions TcdB¹⁻⁵⁰⁰ (nucleotides 1-1500), TcdB¹⁻⁴²⁰ (nucleotides 1-1260), TcdB¹⁻¹⁷⁰ (nucleotides 1-510), TcdB³⁵⁻⁵⁵⁶ (nucleotides 103-1668), TcdB⁶⁷⁻⁵⁵⁶ (nucleotides 202-1668) were PCR amplified using primers listed in Table 1 and cloned into the BamHI site of pABII to make the plasmids pLMS201, pLMS202, pLMS204, pLMS205, and pLMS206 respectively. Following ligation, the mixture was transformed into *E. coli* XL1-blue (Stratagene, La Jolla, CA) and screened for inserts. Candidate clones were then transformed into *E. coli* BL-21(DE3) (Stratagene), BL-21 (DE3) Star (Invitrogen), or BL21 (DE3) RIL (Stratagene) for expression.

Table 1. Primer Sequences For LFnTcdB enzymatic domain and deletion mutants.

Carboxy-terminal deletions

<u>Name</u>	<u>Primer sequence</u>	<u>Amino Acids coded for</u>
-------------	------------------------	------------------------------

Forward primer

pTB1	ggccggggatccatgagtttagttaatagaaaa	
------	-----------------------------------	--

Reverse primer

pTBJB02ba556	gccggggatccgtttcttaaatacagcttctatc	1-556
--------------	------------------------------------	-------

pTBJB02ba	gccggggatccgtttcttaaatacagcttctatc	1-500
-----------	------------------------------------	-------

TCDB420	ggcgccggatccttactcgctaatactggattaa	1-420
---------	------------------------------------	-------

TCDB170	ggcgccggatccttatgtgtttatcaaaaatgcatt	1-170
---------	--------------------------------------	-------

Amino-terminal deletions

<u>Name</u>	<u>Primer sequence</u>	<u>Amino Acids coded for</u>
-------------	------------------------	------------------------------

Forward Primers

LFnTbF 100	taccggggcataatatgtcagagaataact	34-556
------------	--------------------------------	--------

LFnTbF 200	taccgggggtagaataaagccttaaaaa	67-556
------------	------------------------------	--------

Reverse Primer

pTBJB02ba556	gccggggatccgtttcttaaatacagcttctatc	
--------------	------------------------------------	--

Site directed mutants

Site directed mutants were generated using Pfu Turbo DNA polymerase and the QuickChange mutagenesis approach (Stratagene). Oligonucleotides for generation of TcdB1-556_{C365S}, TcdB1-556_{C365W}, and TcdB1-556_{W102A} are listed in table 2. Mutants were selected in *E. coli* XL1 blue and confirmed by sequencing, followed by transformation into *E. coli* BL-21 Star for expression.

Expression and isolation of recombinant RhoA, Rac1, and Cdc42 substrates and PA

RhoA, Rac1, and Cdc42 were expressed from a pGEX2-T plasmid kindly provided by Dr. Alan Hall (University College London), and purified on a GST column. Briefly, 1L cultures were induced with 1 mM IPTG for 4 h at 37°C. Cells were harvested by centrifugation, resuspended in 30 ml PBS and lysed by sonication in the presence of a protease inhibitor cocktail containing TLCK (Na-p-tosyl-l-lysine chloromethyl ketone), TPCK (L-1-tosyl-amide02-phenylmethyl chloromethyl ketone), and phenylmethylsulfonyl fluoride (Sigma Chemical). One milliliter of GST resin (Amersham Pharmacia) was washed three times in 1 ml PBS and incubated with the clarified cell extract shaking gently for 30 minutes at room temperature. The mixture was then added to a Bio-Rad poly prep column. The column was washed with 15 ml PBS and the fusion protein was eluted with 1.5 ml reduced glutathion elution buffer. Protein concentrations were determined by the Bradford assay (Bio-Rad Laboratories).

Table 2. Primers for Site-directed Mutagenesis.

<u>Name</u>	<u>Primer sequence</u>	<u>Amino Acids modified</u>
Sense C365S1	gtttactattaaattgctagaatatgagtccttcacag	
Antisense C365S2	ctgtgaaagactcatattctagcaatttaatagtaaaac	Cysteine 365 to Serine
Sense C365W1	gtttactattaaattgctaccatatgagtccttcacag	
Antisense C365W2	ctgtgaaagactcatattggagcaatttaatagtaaaac	Cysteine 365 to Tryptophan
Sense W102A1	aaaaatttacattttgttgctattggaggtcaa	
Antisense W102A2	ttgacctccaatagcaacaaaatgtaaattttt	Tryptophan 102 to Alanine

Recombinant PA was isolated from *E. coli* BL-21, harboring the plasmid, pSRB/ET-15b-PA (a generous gift from Steven Blanke). Expression was induced with 100 μ M IPTG for 12 h at 16°C, and the His-tagged protein was purified using His Bind Quick columns (Novagen) according to the manufacturer's instructions. Imidazole was removed from the eluted protein using PD10 desalting columns (Amersham Pharmacia), according to the manufacturer's instructions. Protein concentrations were determined by the Bradford assay (Bio-Rad Laboratories).

Isolation of LFnTcdB Fusion Proteins

LFnTcdB₁₋₅₅₆, LFnTcdB₁₋₅₀₀, LFnTcdB₁₋₄₂₀, LFnTcdB₁₋₁₇₀, LFnTcdB₃₅₋₅₅₆, LFnTcdB₆₇₋₅₅₆, LFnTcdBC365S, LFnTcdBC365W, and LFnTcdBW102A were expressed in *E. coli* strain BL-21 Star grown in Luria broth (1.0% trypton (w/v), 0.5% yeast extract (w/v), and 1.0% NaCl) supplemented with 75 μ g/ml ampicillin. Expression was induced by the addition of 100 μ M IPTG to cultures at a density between 0.6 and 0.8 OD₆₀₀ units. Following a 12 h induction at 16°C, cells were harvested by centrifugation and resuspended in His bind buffer (5mM imidazole, 150mM NaCl, 20mM Tris (pH 7.9)), and lysed by sonication. Both LFn and the LFnTcdB fusion proteins were isolated using a nickel resin column, following the manufacturer's instructions (Novagen). Inclusion body purification was also performed according to the manufacturer's instructions (Novagen). One change was made to the manufacturer's protocol. LFnTcdB fusion proteins partially eluted in the recommended 60 mM imidazole wash buffer, so columns were washed with buffer containing 40 mM imidazole instead. As a second purification

step, the protein was resolved on a high-resolution anion exchange (mono-Q) column at a flow rate of 1 ml/min in a buffer containing 20 mM Tris (pH 8.0). LFnTcdB fusions were eluted using a linear gradient from 0-100% NaCl and collected in 1 ml fractions. The fractions were analyzed by SDS- PAGE and by immunoblotting with an anti-His antibody (Santa Cruz Biotechnology Inc) and a HRP-conjugated secondary antibody.

Immunoblots were performed by loading 5 μ l of candidate fractions onto a 10% SDS-acrylamide gel, and electrophoresing at 200 V for 40 min. The proteins were then transferred to a 0.45 μ m nitrocellulose membrane (BioRad Laboratories) soaked in transfer buffer (190mM Glycine, 25mM Tris, .01% SDS, and 20% (v/v) methanol), using a BioRad transblot SD semi-dry transfer cell set at 20 V for 1 h. Following transfer, membranes were rinsed for 5 min in TBS buffer (20mM Tris (pH 8.0), and 0.8% sodium chloride) then incubated in a blocking solution containing 20 mM Tris (pH 8.0), 0.8% NaCl, 3% (w/v) non-fat dry milk for 1 hour at room temperature. The membrane was rinsed briefly in TBS containing 0.1% tween 20 (TBST) followed by a 1 h incubation with primary antibody (α His) (Santa Cruz Biotechnology, Santa Cruz, CA) diluted 1/1000 in TBST. The blot was washed in 100 ml TBST with 5 changes of wash buffer for a total of 35 min. Horseradish peroxidase secondary rabbit antibody was diluted 1/10,000 in blocking solution and allowed to incubate for 1 h at room temperature. The membrane was then washed as described above, and the blot was developed using luminol reagent (Santa Cruz Biotechnology) according to the manufacturer's instructions. Blots were exposed to BioMax MR film (Kodak) for between 10 s and 5 min and the film was developed using GBX developer and fixer (Kodak) according to the manufacturer's

instructions. Fractions containing the fusion were pooled and tested for PA dependent cytopathic effects on CHO cells.

Glucosylation assay

CHO cell extracts and GST-RhoA, GST-Rac1, and GST-Cdc42 were used as substrates to test glucosylation by TcdB¹⁻⁵⁵⁶, TcdB¹⁻⁵⁰⁰, TcdB¹⁻⁴²⁰, TcdB¹⁻¹⁷⁰, TcdB³⁵⁻⁵⁵⁶, and TcdB⁶⁷⁻⁵⁵⁶ and TcdB. In order to prepare these extracts, CHO cells were grown in 75 cm² tissue culture flasks until confluent. The cells were then washed three times in ice cold PBS followed by mechanical removal (scraping) in the presence of lysis buffer (1 mM MgCl₂, 1 mM MnCl₂, 0.1 mM phenylmethylsulfonyl fluoride (PMSF) 10 µg/ml leupeptin, 25 mM triethanolamine-HCl (pH 7.5)) similar to a previously described method (Just et al., 1994). Cells were sonicated on ice 5 times for 30 s intervals and the resulting extract was centrifuged at 40k x g for 8 h. The supernatant was removed and concentrated in a Centricon concentrator with a 10 kD mwco (Millipore) until the extract reached a final volume of 0.5 ml.

CHO extracts (10 mg/ml), GST-RhoA, GST-Rac1, or GST-Cdc42 (1 mg/ml) were added to a glucosylation mix containing 50 mM HEPES, 100 mM KCl, 1 mM MnCl₂, 1 mM MgCl₂ 100 µg/ml BSA, 20 mM [¹⁴C]UDP-glucose (308 Ci/mol; ICN Pharmaceuticals Inc) and 25 ng (96 fmol) TcdB or 200 ng (~2 pmol) of the indicated LFnTcdB fusion in a final reaction volume of 20 µl. The reaction was incubated for two hours at 37°C and resolved by SDS-PAGE on a 15% acrylamide gel and imaged on a Packard electronic autoradiograph instant imager (Packard Instrument Company) similar to previously

described methods (Just et al., 1994; Wagenknecht-Wiesner et al., 1997; Hoffman et al., 1997).

For differential glycosylation assays, HeLa cells (1×10^7) were first treated with 325 pmol of PA and 2.5 nmol of each fusion protein in a T-75 tissue culture flask with a final volume of 20 ml. Following 16 h treatments, cells were washed 3 X in ice-cold PBS, scraped and extracts were prepared as described above for glycosylation extracts.

Cytotoxicity assay and mouse lethality

CHO cells were plated at a concentration of 3×10^4 cells/well in 96 well microtiter plates. The cells were allowed to adhere overnight and were then used to test the ability of LFnTcdB fusions to target cells in the presence and absence of PA. LFnTcdB fusion protein (6.25 pmol) was added to each well. A fixed amount of PA (3 pmol) was added to each of the PA containing wells. Each sample was performed in triplicate and cytopathic effects were determined by cell rounding.

In order to test for lethal effects of LFnTcdB¹⁻⁵⁵⁶ in BALB/c mice, ten fold dilutions of the fusion plus 3 pmol PA were added to CHO cells grown in a 96 well plate. The amount of fusion required to cause cytopathic effects in 50 percent of cells after 12 hours was determined to be the tissue culture infectivity dose (TCID₅₀). A test group consisting of 4 mice was injected intravenously with 1, 10, 100, or 1000 TCID₅₀ and 30 pmol of PA.

Actin Cytoskeleton Staining

Human lung fibroblast cells were grown on glass coverslips in 24-well culture dishes in complete medium (minimum essential medium with high glucose [Gibco BRL], 200 U of penicillin/ml, and 200 µg of streptomycin/ml) until semi-confluent. To determine if PA plus LFnTcdB¹⁻⁵⁵⁶ induces actin condensation similar to that induced by TcdB, the cells were treated with 2 TCID₅₀s TcdB or LFnTcdB¹⁻⁵⁵⁶ and 3 pmol PA for four hours. Controls of PA alone and LFnTcdB¹⁻⁵⁵⁶ in the absence of PA were also tested. The treated cells were fixed for 20 min in fresh 2% paraformaldehyde in 20 mM HEPES (pH 7.5), with 150 mM NaCl. The cells were then washed once with PBS, permeabilized for 10 min with 0.1% Triton X-100 in PBS at 4°C, then washed three more times with PBS. The cellular actin filaments were stained by incubating the permeabilized cells with a 1:40 dilution of rhodamine phalloidin (Molecular Probes) for 30 min at room temperature, and washing three times with PBS. The cells were mounted in glycerol:PBS/azide (8:1), and analyzed using an AX-70 microscope equipped with epifluorescence optics (Olympus America, Inc.). A Spot cooled digital camera was used to capture the images (Diagnostic Instruments, Inc.).

Hydrolase assays

Glucosylhydrolase assays were carried out in a reaction mix containing 50 mM HEPES, 100 mM KCl, 1 mM MnCl₂, 1 mM MgCl₂, 100 µg/ml BSA, 0.2 mM GDP, 40 µM [¹⁴C]UDP-glucose (303 Ci/mol; ICN pharmaceuticals Inc.) 100 µM UDP-glucose and 3 pmol of TcdB or 10 pmol of each fusion protein in a total volume of 25 µl. The assay

was allowed to incubate overnight at 37°C, similar to a previously described protocol [47], and the cleaved UDP-glucose was separated using AG1-X2 anion exchange resin. The column was washed with 4 ml ddH₂O and 100 µl of each wash was counted in a liquid scintillation counter. One microliter of the reaction was collected before separation on the column and counted in a liquid scintillation counter. The percent of UDP-glucose cleaved was determined by using the following equations.

The total counts present in the hydrolase reaction were determined using the following equation:

$$C \times V = T_c$$

where C = counts in 1 µl of the original reaction, V = volume of the reaction (25 µl), and T_c = total counts present in the reaction.

The number of counts present in the wash was determined by the following equation:

$$C_w \times V_w / V_c$$

where C_w = counts from the wash sample, V_w = volume of the wash (4,000 µl), and V_c = volume counted (100 µl).

Finally, the percentage of UDP-glucose cleaved was determined by dividing the counts from the wash (C_w) by the total counts present in the reaction (T_c).

Each value was determined by averaging duplicate reactions.

Inhibitor assays

For the inhibitor assay, HeLa cells were plated in 96 well microtiter plates (3×10^4 cells/well) and allowed to incubate overnight. The following day the cells were treated with 4 pmol of the appropriate LFnTcdB fusion plus 8.5 pmol of PA in a final volume of 100 μ l. The cells were cotreated with 80 fmol of TcdB and observed for cytopathic effects. For sustained inhibition assays, 30 pmol of LFnTcdB¹⁻⁵⁰⁰ plus 8.5 pmol of PA were added to cells in a final volume of 100 μ l and allowed to incubate 30 min, at which point 20 fmol of TcdB was added to the cells. Following the initial treatment, 30 pmol of LFnTcdB¹⁻⁵⁰⁰ and 8.5 pmol of PA were added every 30 min for the first 90 min and every hour thereafter up to 12 h. Wells treated with TcdB alone were amended with an equivalent volume of buffer each time inhibitor treated cells were amended. The cells were observed for cytopathic effects for an additional 18 h. Similar competition assays were carried out using 2 pmol of TcsL or 300 ng of *C. difficile* culture supernatant. For inhibition assays with TcsL, cells were subjected to a brief acid-pulse, which enhances cytotoxic activity for this toxin. For the TcsL inhibition assay, cells were treated with TcsL via an acid pulse as previously described [48]. Briefly, LFnTcdB¹⁻⁵⁰⁰ was added to cells, allowed to incubate for 20 min then TcsL was added to cells and allowed to incubate for 5 min. The media was removed, replaced with media pH 4.0, and allowed to incubate for 5 min at which time the media was removed and replaced with pH 7.0 media. The cells were amended with 30 pmol of LFnTcdB¹⁻⁵⁰⁰ and 8.5 pmol of PA. The inhibitor was added every 30 min for 90 min, then every hour afterward for 12 h. TcsL

control wells were amended with an equal volume of buffer each time inhibitor was added and CPE were observed 16 h after treatment.

Protection of CHO cells expressing LFnTcdB¹⁻⁵⁵⁶

A CHO cell line was obtained from Dr. William Ortiz-Leduc and used to test for inhibition inside the cell. Briefly, this cell line was constructed by inserting a DNA sequence encoding the enzymatic domain of TcdB (amino acids 1-556) into the multiple cloning site of plasmid pGene/V5-His version B downstream of a Kozak sequence (Invitrogen). The plasmid was linearized with SapI and introduced into GeneSwitch-CHO cells (Invitrogen) by lipofection according to the protocol supplied with the LipofectAMINE PLUS Reagent Kit (Gibco Life Technologies). Transfected cells were selected for using Ham's F12 media plus zeocin (300µg/ml) and hygromycin (100µg/ml). The cells were diluted and plated in 96-well plates. Only wells containing single foci were subcultured in 12-well plates using selective media. GeneSwitch-CHO pGene/TcdB1-556, a lineage of transfected cells showing nearly 100% rounding in 24 h in the presence of mifepristone, was identified and chosen for the experiments reported herein.

GeneSwitch CHO cells transfected with pGene TcdB¹⁻⁵⁵⁶ were plated at 3×10^4 cells per well in 96 well plates in Ham's F-12 media. Cells were allowed to adhere for 6 hours then supplemented with 300µg/ml zeocin and 100µg/ml hygromycin. Six hours after the addition of antibiotics, the cells were treated with mifepristone (10^{-8} M) in order to induce

expression of the TcdB enzymatic domain. Two hours after the induction, before cytopathic effects were observed, 8.5 pmol PA and 30 pmol LFnTcdB¹⁻⁵⁰⁰ or an equal volume of buffer (control wells) were added to cells. The treatments were repeated every 30 min for up to 6 hours and the percent CPE were recorded for duplicate wells with and without PA, LFnTcdB¹⁻⁵⁰⁰.

In vitro Inhibition experiments

In vitro glucosylation was carried out in a reaction mix as described above for glucosylation assays. TcdB (25 fmol) was added to the reaction mix containing HeLa cell extract (1.8 mg/ml) in a final reaction volume of 25 μ l. LFnTcdB¹⁻⁵⁰⁰ (5.2 pmol) was added to one assay while an equal volume of buffer was added to a second assay. The reactions were incubated for 25 minutes and run on a 15% polyacrylamide gel. The gel was dried and exposed to film for 5 days.

Differential glucosylation of HeLa extracts from cells cotreated with LFnTcdB¹⁻⁵⁰⁰ and TcdB

HeLa cells were plated in T-25 tissue culture flasks and allowed to incubate until semi-confluent. LFnTcdB¹⁻⁵⁰⁰ (26 nmol) and PA (30 pmol) were added to cells and allowed to incubate for 30 minutes. TcdB (190 fmol) was added to the cells in the presence and absence of the inhibitor. The cells were allowed to incubate until those lacking inhibitor became 40% round (approximately 3 hours). Extracts were then prepared and used as a source of substrate for in vitro glucosylation assays.

V8 protease digestion

LFnTcdB¹⁻⁵⁵⁶, LFnTcdB^{W102A}, and LFnTcdB^{C365W} (2 µg) were digested with 10 ng V8 protease for 1 or 2 h. The digestions were run on a 15% acrylamide gel and immunoblotted using a primary α His antibody according to the protocol described previously.

RESULTS

Time Course of cytosolic entry for TcdB and TcsL

In order to determine the time course of cellular entry for TcdB, CHO cells were treated with TcdB followed by the addition of the lysosomotropic inhibitor bafilomycin A1 at 10 min intervals. Bafilomycin blocks acidification of the endocytic vesicle preventing TcdB from translocating into the cytosol and gaining access to cellular targets. Cells were partially protected from TcdB induced cytopathic effects by the addition of Bafilomycin A1 up to 50 minutes following TcdB treatment. Small amounts of TcdB began to enter the cytosol after 40-50 min indicated by the 40% CPE observed at 8 hours post treatment, however, CPE comparable to the TcdB control did not occur until 60 min post treatment (Figure 8). A similar experiment was performed using a related LCT, TcsL. TcsL treated cells were still 60 % protected from CPE when bafilomycin was added even 120 min after the addition of toxin (Figure 9). This indicates that TcdB is much more efficient at binding and entering into CHO cells than TcsL.

Purification of the TcdB enzymatic domain fused to LFn (LFnTcdB¹⁻⁵⁵⁶)

The amino-terminal 556 amino acids of TcdB, which encompasses the glucosylating domain of TcdB, was fused to the amino-terminal 254 residues of LF (LFn), expressed in *E. coli* BL-21 (DE3) and purified using an amino terminal hexa-His tag. This fusion consistently eluted at 60-80 mM imidazole compared to LFn, which eluted at 250 mM

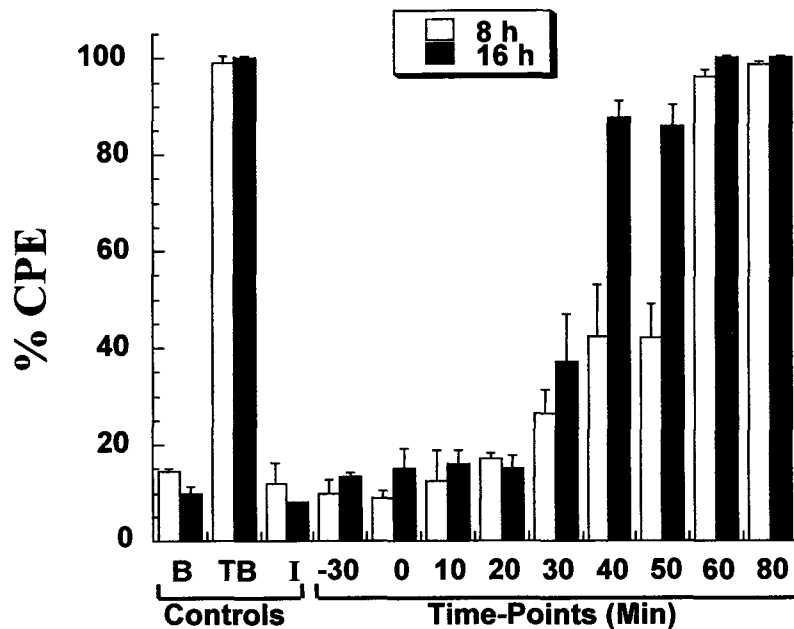


Figure 8. Bafilomycin A1 inhibition of TcdB Cytosolic Entry. 200 fmol of TcdB was added to CHO cells in a 96 well plate. Bafilomycin (5×10^{-7} M) was added every 10 minutes following TcdB treatment. Samples were performed in triplicate and error bars mark the standard deviation. CPE were recorded after 8 and 16 hours. B, buffer control; TB, TcdB alone; I, inhibitor only.

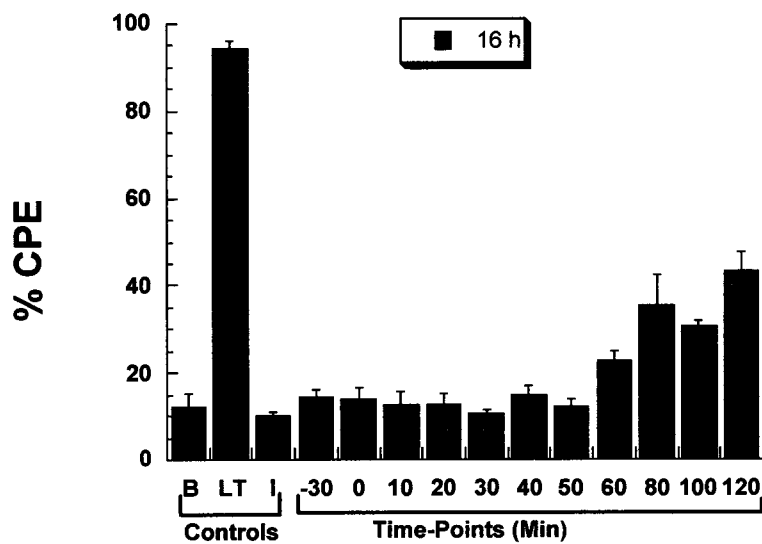


Figure 9. Bafilomycin A1 inhibition of TcsL cytosolic entry. TcsL (1 pmol) was added to CHO cells plated in a 96 well plate. Bafilomycin A1 was added to cells at the indicated times after TcsL treatment. CPE were recorded after 16 hours. B, buffer control; LT, TcsL alone; I, inhibitor alone. Samples were performed in triplicate and error bars mark the standard deviation.

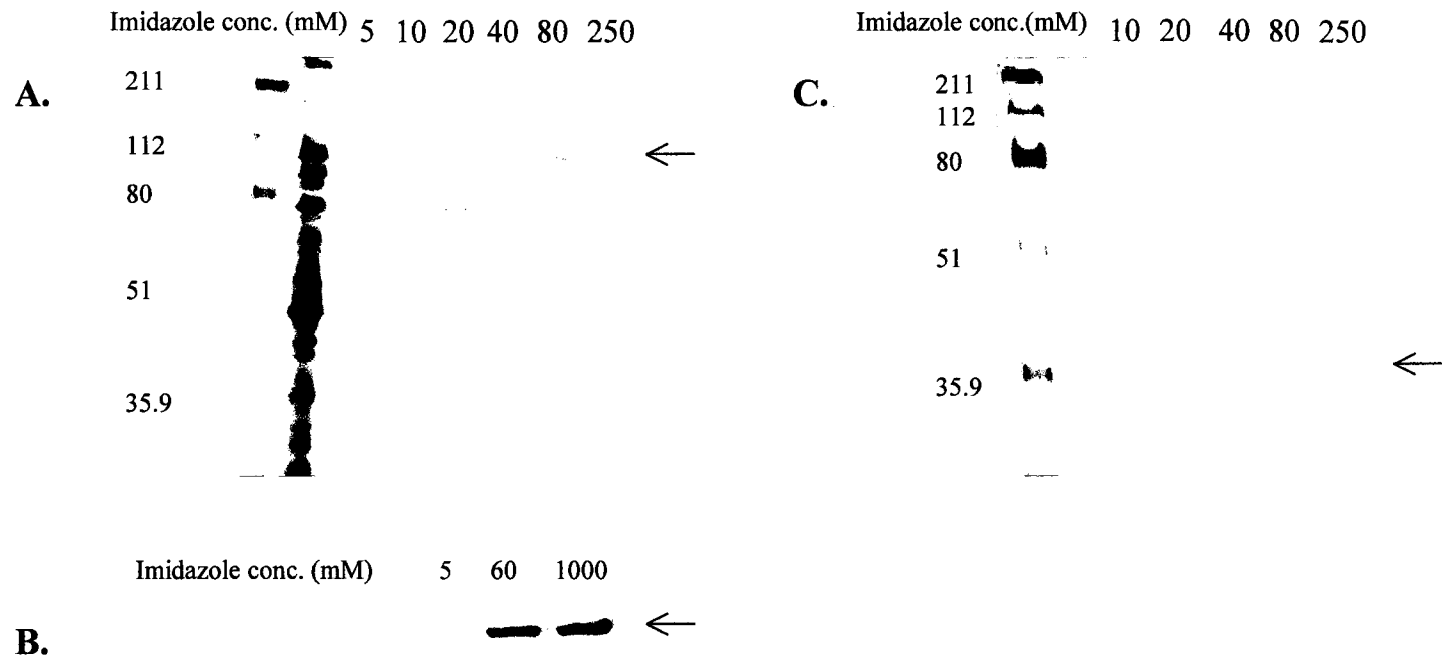


Figure 10. Nickel Column Purification of LFnTcdB¹⁻⁵⁵⁶ and LFn. A. LFnTcdB¹⁻⁵⁵⁶ purification Lane 1, molecular weight markers; Lane 2, flow through; Lanes 3-8; washes with indicated concentration imidazole. B. LFnTcdB¹⁻⁵⁵⁶ purification using the standard 60 mM wash buffer and 1 M elution buffer. C. LFn purification Lane 1, molecular weight markers; Lane 2, flow through; Lanes 3-7; washes with indicated concentration imidazole. LFnTcdB¹⁻⁵⁵⁶ eluted at 60-80 mM imidazole, whereas LFn eluted at 250 mM imidazole. Arrows indicate the correct size of the fusion and LFn

imidazole suggesting the His tag may only be partially exposed in the LFnTcdB fusion (Figure 10). Furthermore, protein yields were about 1-2 mg/L of purified protein and co-purifying truncated forms were common.

Several methods were employed to enhance expression of LFnTcdB¹⁻⁵⁵⁶. The fusion protein was expressed at 16°C. Some target proteins express more efficiently at lower temperatures and it has been suggested that this phenomenon is a result of increased solubility of the target protein at the lower temperature. Additionally, many cytosolic proteases are active at 37°C, but inhibited at 16°C, and the lower temperature may improve expression of the target protein by preventing proteolysis. An immunoblot of purified LFnTcdB¹⁻⁵⁵⁶ after a 12 h induction at 16°C did indicate that truncated forms of the purified fusion protein were reduced compared to the same protein isolated from a 37°C induction (Figure 11). In order to determine if some of the fusion may be insoluble when expressed at 37°C, a His-tag purification was performed by solubilizing the sonicated cell pellet in nickel column buffers containing 8 M urea. No fusion protein eluted from a column performed under denaturing conditions but all the protein was recovered from the soluble fraction indicating the protein was not present in inclusion bodies.

It has been reported that many genes from gram-positive organisms contain codons that are rare to *E. coli* and therefore result in early termination of transcripts and low protein yields when over expressed in *E. coli* [49]. As an attempt to improve expression of the LFnTcdB¹⁻⁵⁵⁶ fusion protein, the BL-21 (DE3) RIL strain was analyzed. This strain



Figure 11. Immunoblots of Purified LFnTcdB¹⁻⁵⁵⁶ Expressed at 37°C and 16°C. Lane 1, BL-21(DE3) expression at 37°C; Lane 2, BL-21(DE3) expression at 16°C.

contains a plasmid that encodes for extra copies of the *argU*, *ileY*, and *leuW* tRNA.

These tRNA recognize the AGA/AGG, AUA, and CUA codons, respectively. These are codons common to organisms with AT rich genomes such as Clostridia but rare in *E. coli* [50]. When the sequence that encodes for the first 556 amino acids of TcdB was examined, it was determined that AT bases accounted for 70% of the residues and 16 AGA/AGG, 21 AUA, and 2 CUA codons were present indicating that using this strain may improve expression of LFnTcdB¹⁻⁵⁵⁶.

A second strain BL-21 (DE3) Star was also analyzed. This strain has a truncated RNase E gene and has been shown to stabilize mRNA, which may be susceptible to degradation in the BL-21 (DE3) strain. As an additional attempt to improve the amount of full length protein expressed, the plasmid encoding for rare tRNA was isolated from the BL-21 (DE3) RIL strain, transformed into BL-21 (DE3) Star to make the strain BL21 (DE3) Star-RIL. LFnTcdB¹⁻⁵⁵⁶ was expressed in BL21 (DE3) RIL, BL21 (DE3) Star, and BL-21 (DE3) Star-RIL strains and purified using the standard protocol. Immunoblots were performed on freshly isolated LFnTcdB¹⁻⁵⁵⁶ expressed in each of these strains. As can be seen in figure 12, expression in BL-21 Star resulted in a decrease of truncated protein, while the BL-21 RIL strain did not. Furthermore, transformation of BL-21 star with the RIL plasmid did not further reduce the presence of truncated proteins. Based on these initial studies, an approach of expressing the fusion protein at 16°C in the BL-21 Star strain was selected. Additionally, a lower imidazole concentration (40mM instead of the

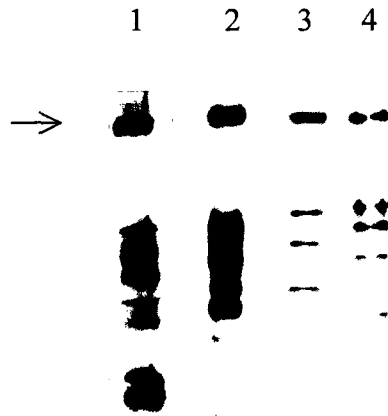


Figure 12. Immunoblots of Purified LFnTcdB¹⁻⁵⁵⁶ Expression in Different Strains of *E. coli*. Lane 1, BL-21(DE3); Lane 2, BL21 RIL; Lane 3, BL21 Star; Lane 4, BL-21 Star RIL. The full length fusion is indicated by an arrow.

recommended 60mM) was used for the nickel column wash buffer to avoid partial elution of the fusion in the wash step.

Analysis of the enzymatic activity of LFnTcdB¹⁻⁵⁵⁶

The LFnTcdB¹⁻⁵⁵⁶ fusion was tested for enzymatic activity and compared with the activity of native TcdB. The first step in substrate modification is hydrolysis of the cosubstrate UDP-glucose. Hydrolysis was tested for by mixing 3 pmol TcdB or 10 pmol LFnTcdB¹⁻⁵⁵⁶ with [¹⁴C]UDP-glucose in a reaction buffer, incubating at 37°C overnight and separating the cleaved glucose using an AG1 X-2 anion exchange column. The percent hydrolysis of cosubstrate was determined by washing the column with water and counting the cleaved [¹⁴C]glucose in a liquid scintillation counter. Ten pmol LFnTcdB¹⁻⁵⁵⁶ maintained hydrolysis activity equivalent to 25% of the activity of the 3 pmol native TcdB (Table 3).

Using purified recombinant substrates (GST-RhoA, GST-Rac1, and GST-Cdc42) substrate specificity was determined for LFnTcdB¹⁻⁵⁵⁶ by in vitro glucosylation. Native TcdB and LFnTcdB¹⁻⁵⁵⁶ showed similar substrate specificity and had the greatest activity with Cdc42, followed by Rac, and then RhoA (Figure 13).

To determine the rate of intoxication of CHO cells, we treated with either 100 fmol of LFnTcdB¹⁻⁵⁵⁶ plus PA or 100 fmol of TcdB and followed over time for CPE. It took approximately 2 h longer for cytopathic effects to be observed with the LFnTcdB¹⁻⁵⁵⁶

Table 3. UDP-Glucosylhydrolase activity of LFnTcdB¹⁻⁵⁵⁶. A reaction mixture containing 3 pmol of TcdB or 10 pmol of LFnTcdB¹⁻⁵⁵⁶ was incubated overnight in the presence of [¹⁴C]UDP-glucose. The reaction mixture was passed over an anion exchange column that specifically binds UDP-glucose, but not cleaved glucose. The wash was counted in a scintillation counter, and hydrolysis expressed as a percent of total [¹⁴C]UDP-glucose present before separation. Each value is an average of duplicate assays

Toxin/Fusion	% Hydrolysis	+/-
TcdB	27.7	0.64
LFnTcdB1-556	6.9	1.02

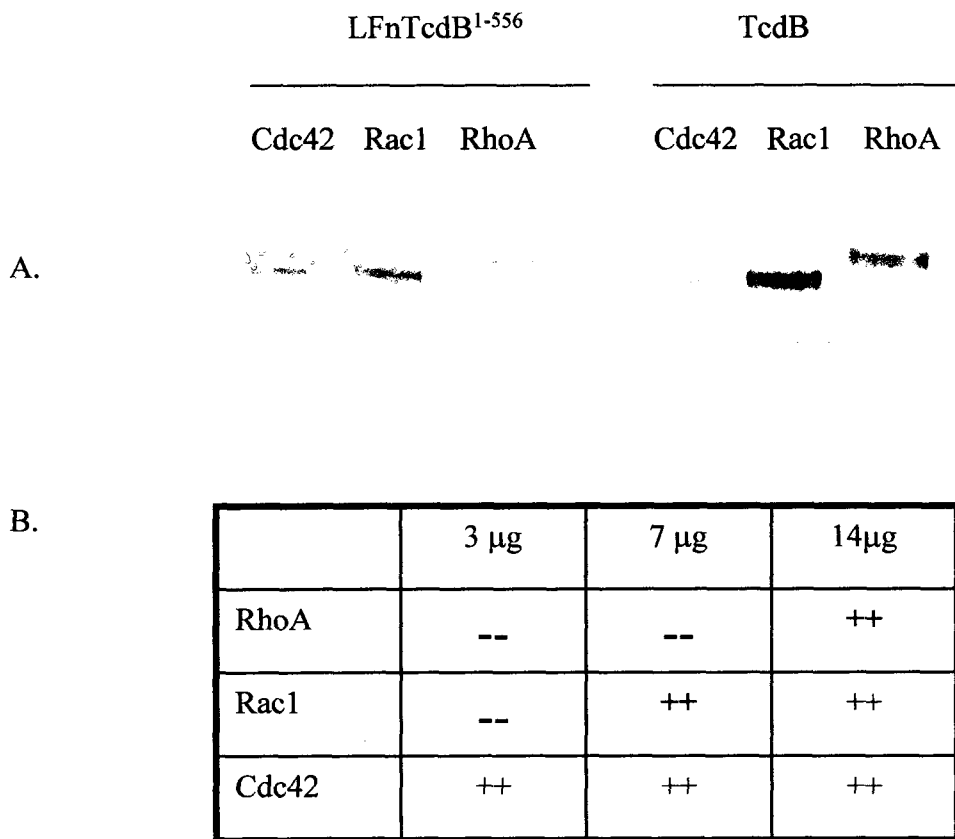


Figure 13. Glucosylation activity of TcdB and LFnTcdB¹⁻⁵⁵⁶. **A.** Recombinant substrates RhoA, Rac1, and Cdc42 (20 μg) were used in an in vitro glucosylation assay with 25 ng TcdB or 200ng LFnTcdB¹⁻⁵⁵⁶. **B.** In order to determine the minimum amount of substrate required for modification under these conditions, substrate concentrations were varied from 3-14 μg. Both the fusion and TcdB preferred Cdc42 as a substrate followed by Rac, and then RhoA. (++) indicates that the substrate was modified by the fusion and by TcdB.

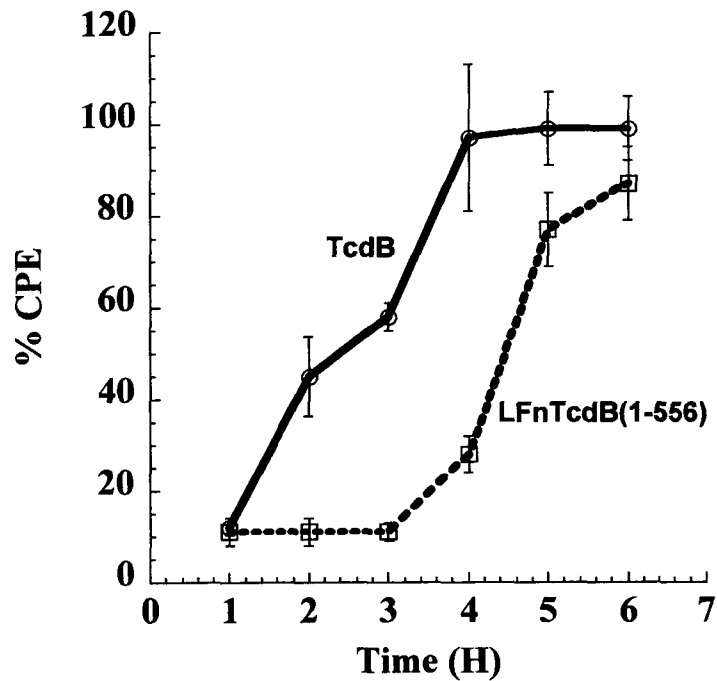


Figure 14. Time-course of CPE for TcdB and LFnTcdB¹⁻⁵⁵⁶ plus PA. CHO cells were plated in 96 well plates (3×10^4 cells/well), allowed to adhere overnight, and treated with TcdB or LFnTcdB1-556 and PA. CPE were determined by cell rounding. Each sample was performed in triplicate. Error bars mark the standard deviation from the mean.

fusion than with native TcdB (Figure 14). Additionally, a dose curve of CPE was performed with TcdB and LFnTcdB¹⁻⁵⁵⁶. It was determined that 100 fold more of the fusion was required to elicit the same CPE as TcdB (Figure 15). The slower cytopathic effect of LFnTcdB¹⁻⁵⁵⁶ on CHO cells is likely due to the reduced hydrolase activity of the fusion compared to native TcdB although an effect of differences in binding and cellular entry on toxicity can not be excluded.

In order to determine if LFnTcdB¹⁻⁵⁵⁶ had the same effect as TcdB on actin organization, human fetal lung fibroblast cells were treated with LFnTcdB¹⁻⁵⁵⁶ plus PA or TcdB for 4 hours followed by staining with rhodamine phalloidin. TcdB and LFnTcdB¹⁻⁵⁵⁶ both caused actin condensation in contrast to PA/LFn alone (Figure 16).

The TcdB Glucosylation Domain Confers Lethality

Taking advantage of the PA/LFn delivery system, LFnTcdB¹⁻⁵⁵⁶ was tested for lethality in BALB/c mice. A test group consisting of 4 mice was injected intravenously with 1, 10, 100, or 1000 TCID₅₀ of LFnTcdB¹⁻⁵⁵⁶ plus PA resulting in 100% lethality of mice injected with 1000 TCID₅₀ of LFnTcdB¹⁻⁵⁵⁶ and PA. Mice injected with similar amounts of PA and LFn were unaffected indicating that the glucosylating domain of TcdB is sufficient to cause death in BALB/c mice (Table 4).

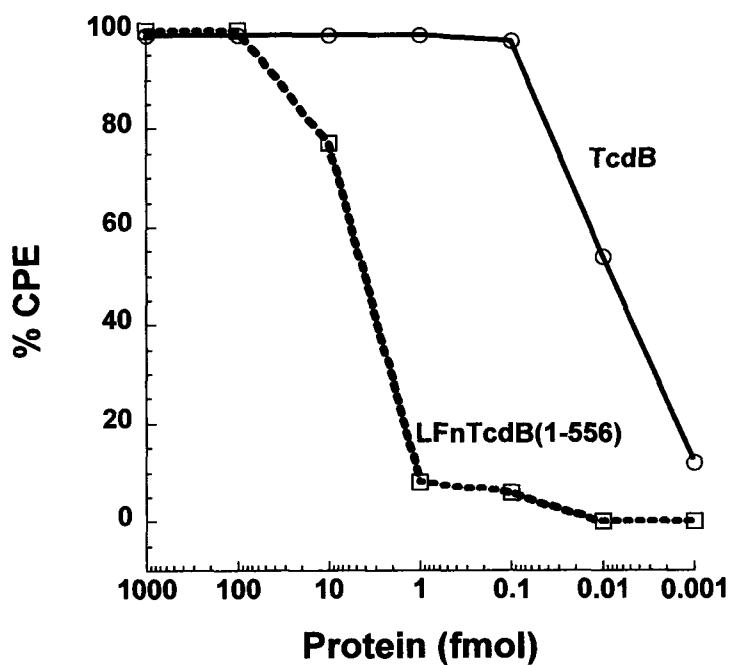


Figure 15. Dose-Curve Response of TcdB and LFnTcdB¹⁻⁵⁵⁶ plus PA CPE. CHO cells were plate (3×10^4 cells/well) in 96 well plates and allowed to adhere overnight. The following day the cells were treated with the indicated amounts of TcdB or LFnTcdB¹⁻⁵⁵⁶ Plus PA. CPE were determined by cell rounding, and were recorded 12 h after treatment.

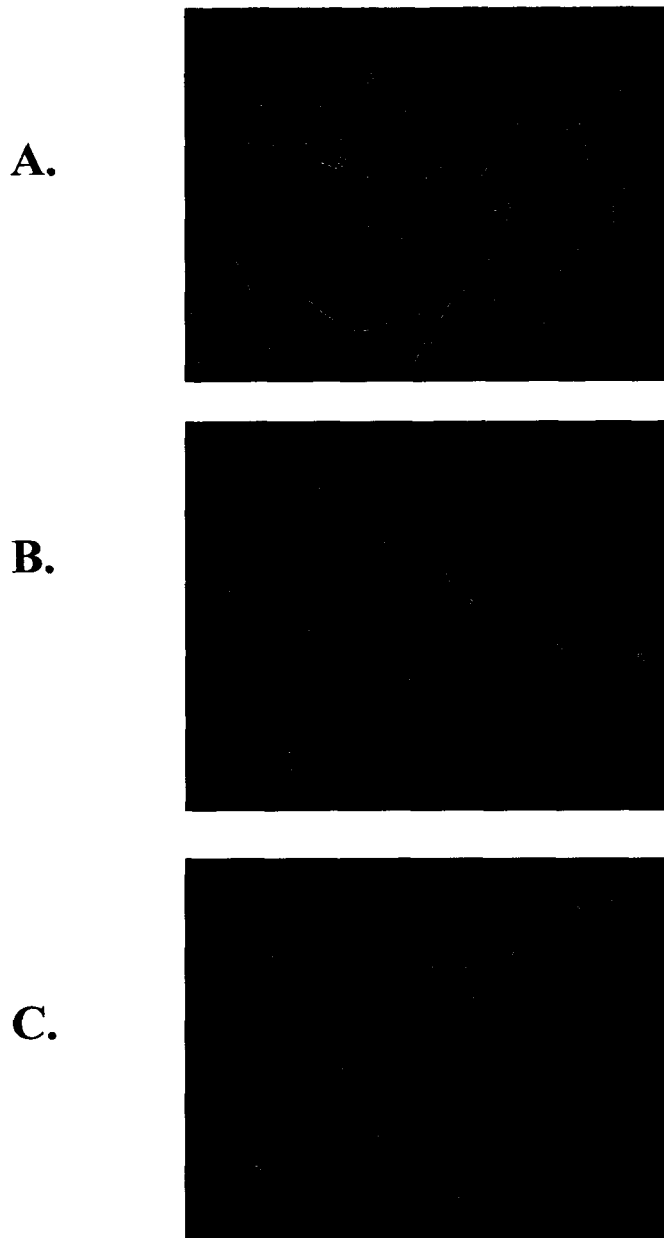


Figure 16. Actin Staining. Fibroblast cells were grown on glass coverslips until semiconfluent and treated with TcdB or LFnTcdB¹⁻⁵⁵⁶ and PA. Cells were stained with Rhodamine phalloidin to visualize F-actin. Panel A, Untreated; Panel B, TcdB; Panel C, PA-LFnTcdB¹⁻⁵⁵⁶.

Table 4. Lethal Effects of LFnTcdB¹⁻⁵⁵⁶. Female Balb/c mice (4/group) were injected intravenously with increasing TCID₅₀ doses of LFnTcdB¹⁻⁵⁵⁶ plus 30 pmol of PA. The correlating TCID₅₀ protein concentrations are shown in column 2. Mice were followed for 18 h after treatment.

TCID ₅₀	LFnTcdB ¹⁻⁵⁵⁶	% Lethality (per 4 mice)
1	0.01 pmol	0%
10	0.1 pmol	0%
100	1.0 pmol	0%
1000	10 pmol	100%

Construction, Purification, and Characterization of Carboxy-terminal Deletions of LFnTcdB¹⁻⁵⁵⁶

Since the LFnTcdB¹⁻⁵⁵⁶ fusion was determined to have similar, although slightly reduced, glucosylation activity as TcdB, a series of mutants of this fusion were generated to further characterize this enzymatic domain. Initially, three fusions with deletions at the carboxy-terminus (LFnTcdB¹⁻⁵⁰⁰, LFnTcdB¹⁻⁴²⁰ and LFnTcdB¹⁻¹⁷⁰) were generated by PCR amplifying each fragment and cloning into the *Bam*HI site of pABII. These fusions were void of glucosylation activity (Figure 17). Since these enzymatically-attenuated mutants may still interact with, but not modify substrate, each of the carboxy-terminal deletions was tested for the ability to inhibit toxicity of native TcdB. Each fusion was added to cells in 96 well plates along with PA and allowed to incubate for 30 minutes, followed by the addition of TcdB. Cytopathic effects were followed over time and it was determined that in the presence of LFnTcdB¹⁻⁵⁰⁰ or LFnTcdB¹⁻⁴²⁰, CPE were delayed for 2 hours suggesting these fusions act as inhibitors of TcdB, while LFnTcdB¹⁻¹⁷⁰ had no inhibitory effect on toxicity of TcdB (Figure 18). To test whether or not the eventual death of cells in the presence of inhibitor could be due to breakdown of the inhibitor within cells, an inhibition assay was set up where inhibitor continued to be added at 30 minute intervals up to 12 hours after the addition of TcdB. Fifty percent of cells treated with TcdB in the presence of the LFnTcdB¹⁻⁵⁰⁰ inhibitor and PA were still protected 36 hours after TcdB addition (Figure 19).

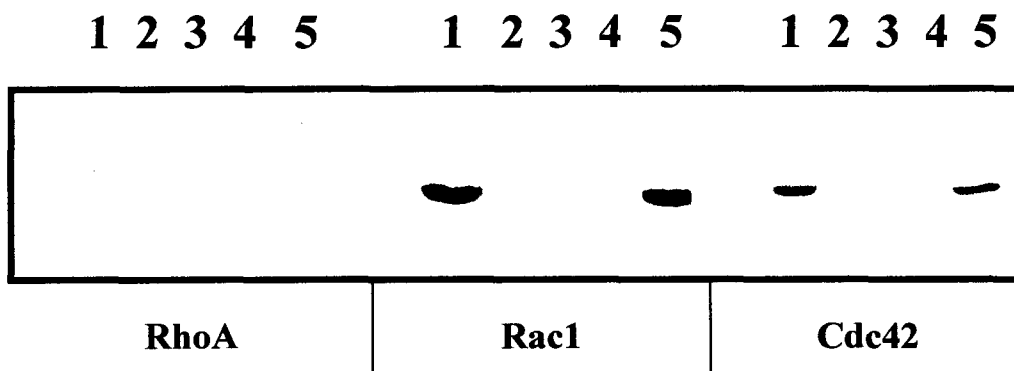


Figure 17. Glucosylation of recombinant substrates RhoA, Rac1, and Cdc42. Lane 1, TcdB; Lane 2, LFnTcdB1-170; Lane 3, LFnTcdB1-420; Lane 4, LFnTcdB1-500; Lane 5, LFnTcdB1-556.

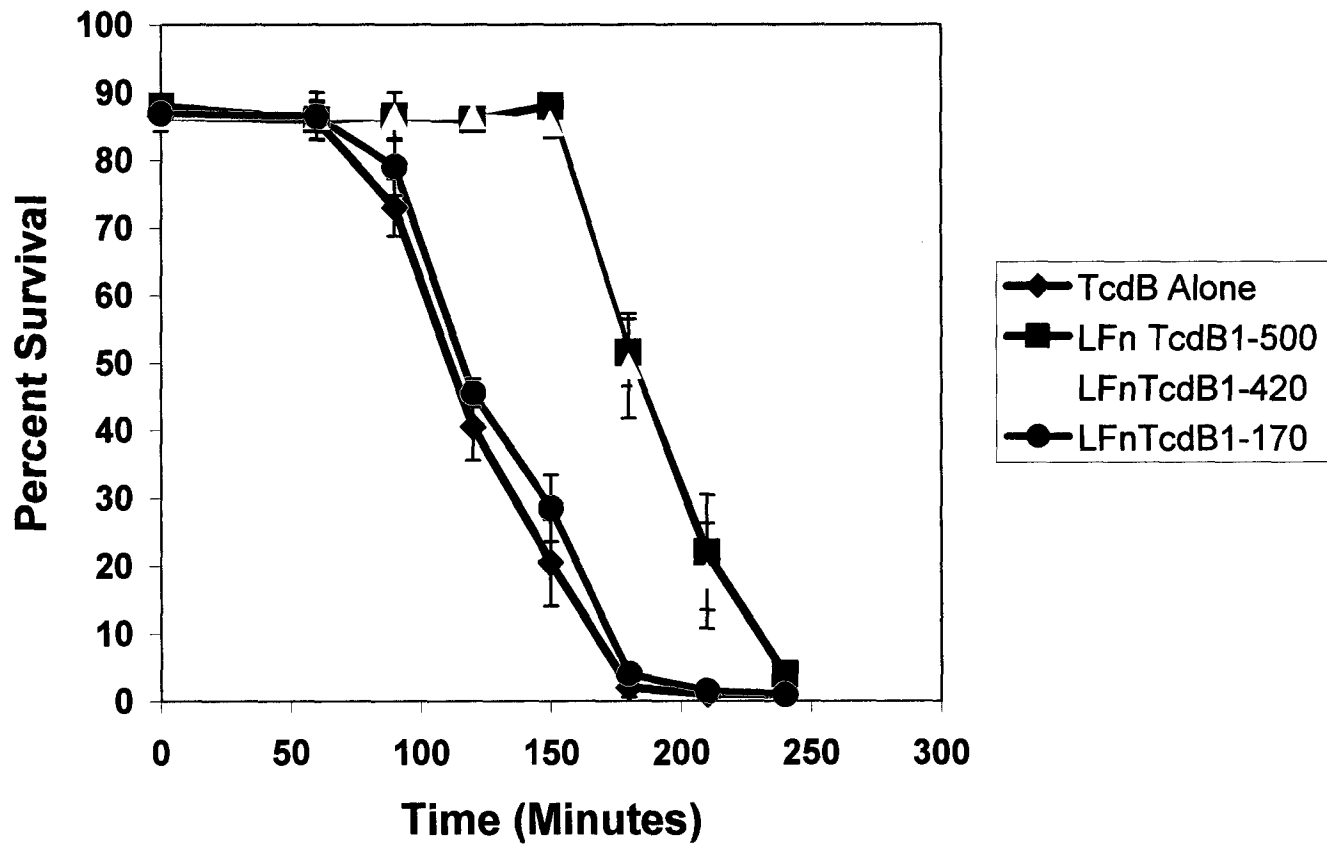


Figure 18. Delayed CPE of TcdB. In the presence of LFnTcdB¹⁻⁴²⁰ and PA or LFnTcdB¹⁻⁵⁰⁰ and PA, TcdB CPE were delayed for approximately two hours compared to TcdB alone or TcdB, LFnTcdB¹⁻¹⁷⁰ and PA. CPE were determined by cell rounding.

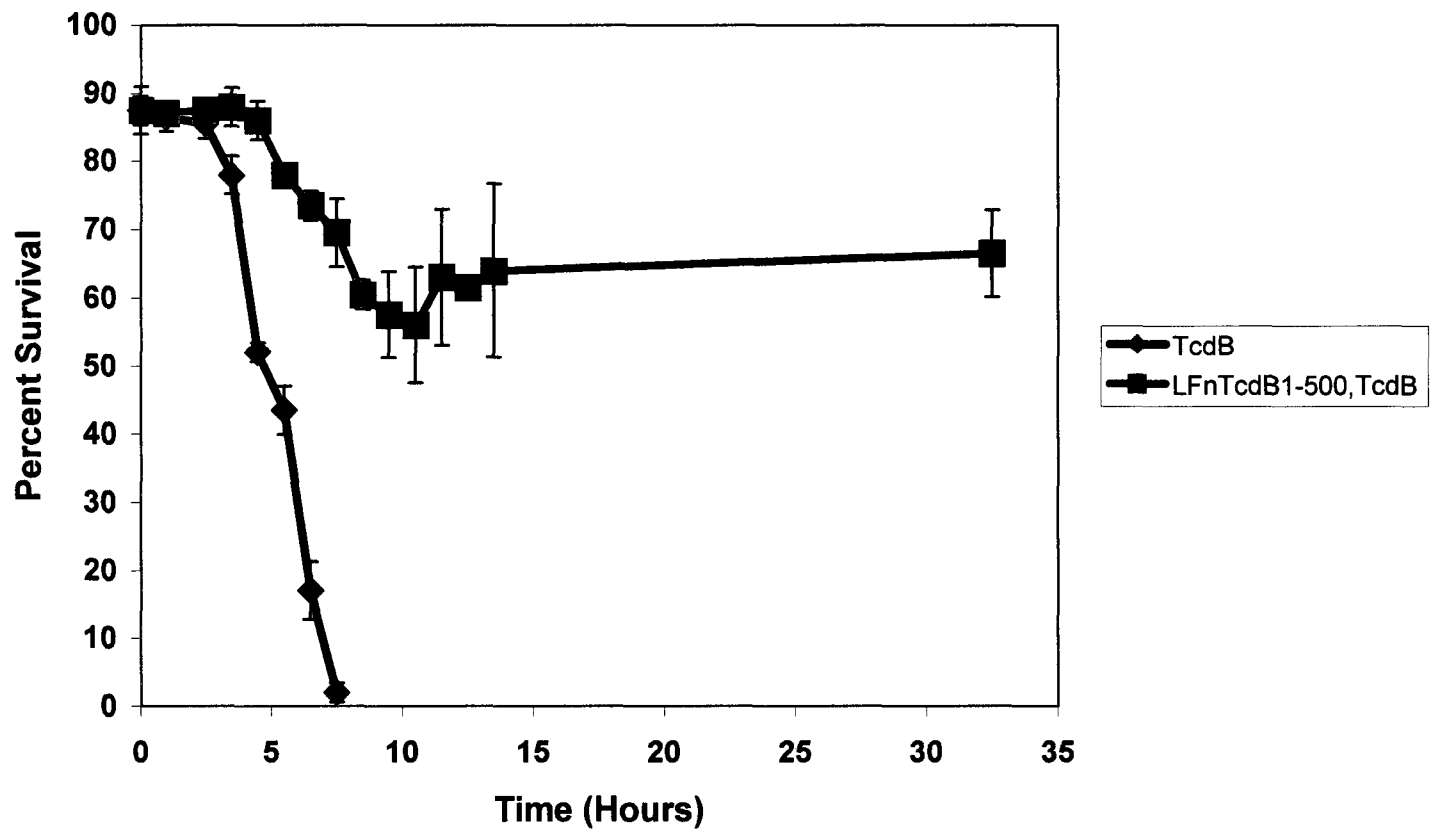


Figure 19. Inhibition of TcdB CPE by the continued addition of LFnTcdB¹⁻⁵⁰⁰. HeLa cells were plated in a 96 well plate (3×10^4 cells/well). The following day the cells were treated with TcdB and LFnTcdB¹⁻⁵⁰⁰ plus PA. During the course of the assay LFnTcdB¹⁻⁵⁰⁰ and PA were added at 30 min intervals for 12 h. The cells were followed for 30 hours and visualized for CPE as determined by cell rounding.

Inhibition of CPE from *C. difficile* supernatant

The therapeutic value of these inhibitors will depend upon their ability to inhibit TcdA as well as TcdB since both toxins are important to the disease process. For this reason, we tested the ability of LFnTcdB¹⁻⁵⁰⁰ to prevent cell rounding when treated with supernatant from a *C. difficile* culture. HeLa cells were cotreated with PA, LFnTcdB¹⁻⁵⁰⁰ and protein from a *C. difficile* culture supernatant. The cells were amended with PA, LFnTcdB¹⁻⁵⁰⁰ every 30 min for the next 12 hours and CPE were determined by cell rounding. Even 28 hours after treatment with the *C. difficile* culture supernatant, 50 percent of cells were protected from toxin induced cell rounding (Figure 20). Since TcdB is 1000 fold more cytotoxic than TcdA and LFnTcdB¹⁻⁵⁰⁰ was not tested for the ability to inhibit the effects of purified TcdA, we cannot conclusively say this protein acts as an inhibitor of TcdA, but it does protect cells from CPE induced by *C. difficile* culture supernatant.

While LFnTcdB¹⁻⁵⁰⁰ was void of hydrolase and transferase activity and showed no cytotoxicity on HeLa or CHO cells, this fragment when administered to cells over a prolonged period of time induced reversible effects on cell shape. That is cells began to condense and take on a more rounded appearance. These cells did not round completely, and when the media was replaced with fresh media, the cells returned to their normal appearance (data not shown).

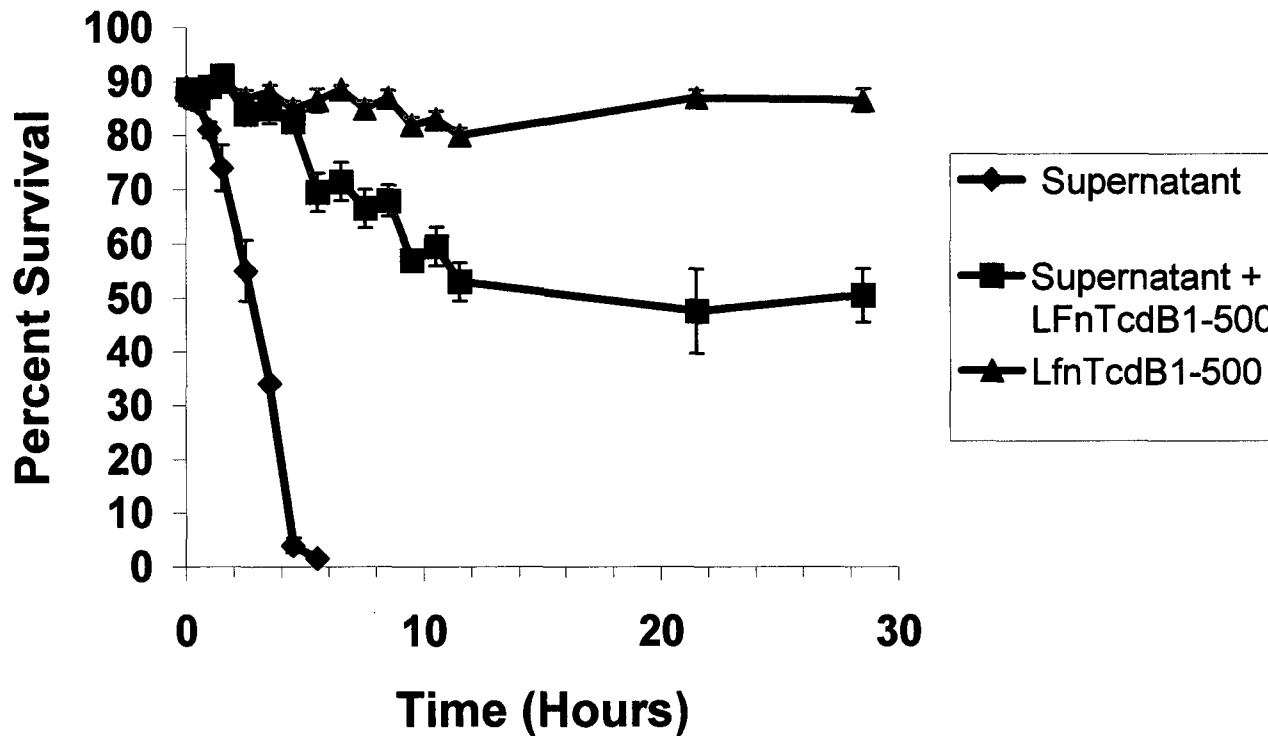


Figure 20. Inhibition of CPE from *C. difficile* supernatant by the continued addition of LFnTcdB¹⁻⁵⁰⁰. HeLa cells (3×10^4 cells/well) were plated in a 96 well plate and allowed to adhere overnight. The following day cells were treated with supernatant from a *C. difficile* culture, or supernatant and LFnTcdB¹⁻⁵⁰⁰ plus PA. LFnTcdB¹⁻⁵⁰⁰ plus PA in the absence of supernatant was added as a control. During the course of the assay LFnTcdB¹⁻⁵⁰⁰ and PA were added at 30 min intervals for 12 h. The cells were followed for 30 hours and visualized for CPE as determined by cell rounding.

Inhibition of *C. sordellii* TcsL

In order to determine if LFnTcdB¹⁻⁵⁰⁰ was able to inhibit the activity of other LCTs, TcsL was purified from *C. sordellii* and introduced into cells via an acid pulse. PA and LFnTcdB¹⁻⁵⁰⁰ were added to cells immediately following the pH pulse and every hour thereafter. Cells were observed for CPE over the next 16 hours. Over 80 percent of cells treated with PA LFnTcdB¹⁻⁵⁰⁰ were protected from TcsL toxicity, while only 40 percent of cells treated with TcsL alone survived the treatment indicating that LFnTcdB¹⁻⁵⁰⁰ can also inhibit toxicity by TcsL (Figure 21).

Inhibition Inside the Mammalian Cell

Inhibition most likely occurs inside the cytosol of cells, however since the receptor for TcdB has not been identified, competition for receptor as a means of inhibition could not be excluded. In order to address the question of whether the inhibition occurs inside the cell, a CHO cell line expressing TcdB¹⁻⁵⁵⁶ under the control of an inducible promoter was utilized. Expression of the enzymatic domain was induced with mifepristone, and two hours later, before the onset of cytopathic effects, the media was removed and replaced with fresh media for control wells or media containing LFnTcdB¹⁻⁵⁰⁰ and PA for test wells. The cells were amended every 30 min for six hours and CPE were recorded in the presence and absence of the inhibitor. LFnTcdB¹⁻⁵⁰⁰ was able to delay CPE by at least 2 hours compared to controls with no inhibitor present (Figure 22). These results indicate that the competition was occurring inside the cell.

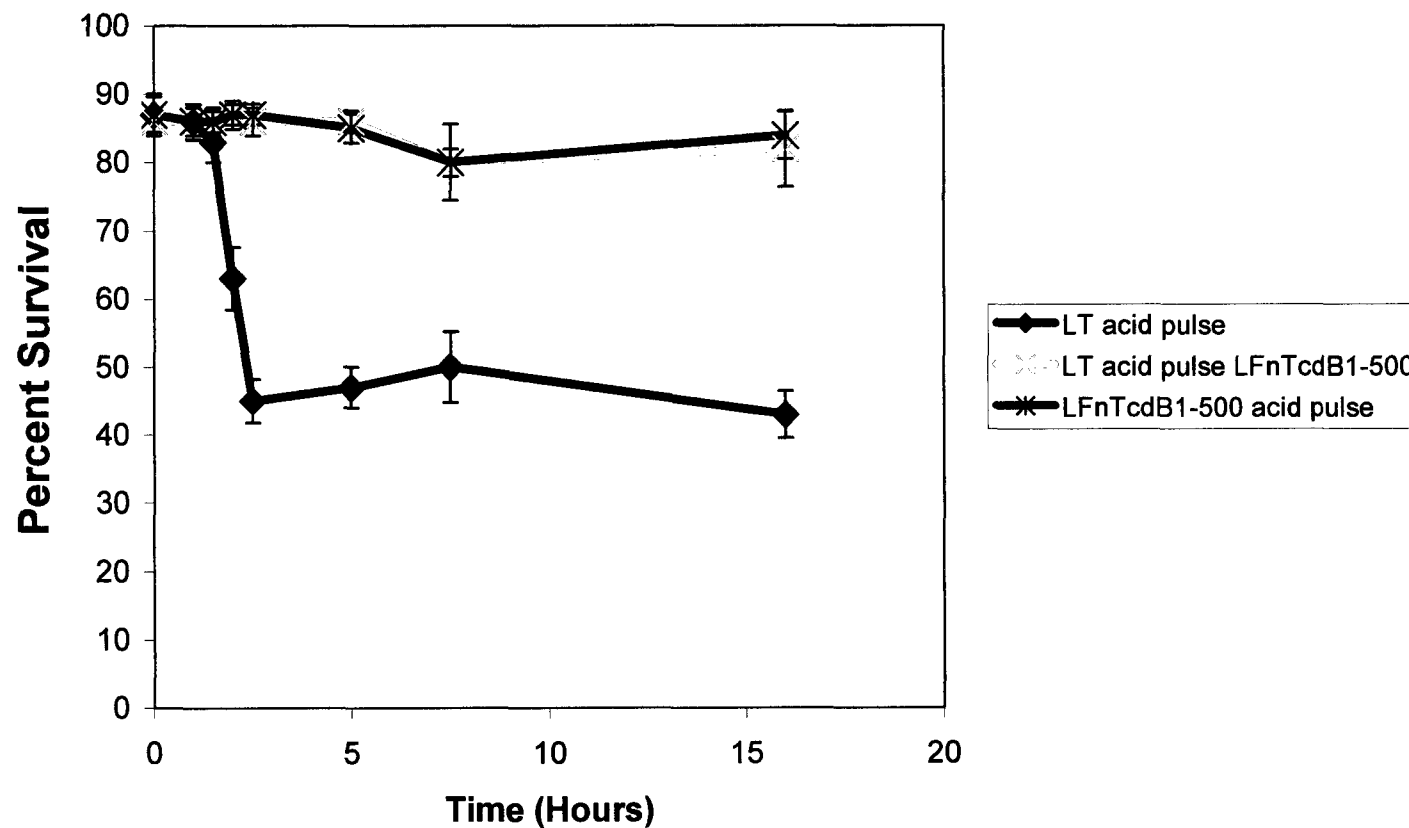


Figure 21. LFnTcdB¹⁻⁵⁰⁰ inhibition of TcsL cytopathic effects. HeLa cells were plated in 96 well plates (3×10^4 cells/well), allowed to adhere overnight, and treated with LFnTcdB¹⁻⁵⁰⁰ plus PA 30 minutes prior to TcsL treatment. TcsL cell entry was mediated via an acid pulse and cells were amended with PA and LFnTcdB¹⁻⁵⁰⁰ immediately and at 30 min intervals for up to 12 hours. Cells were observed for CPE (determined by cell rounding) 18 hours after toxin treatment.

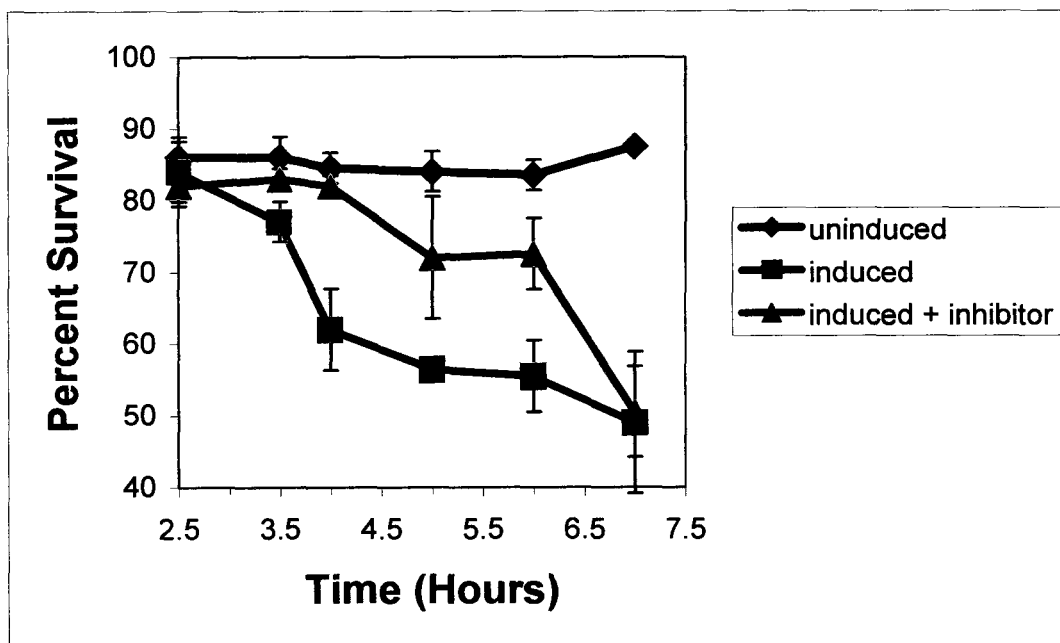


Figure 22. Inhibition of CPE in CHO cells expressing the enzymatic domain of TcdB. A CHO cell line transfected with TcdB¹⁻⁵⁵⁶ under the control of an inducible promoter was induced with mifepristone. 2.5 hours after induction, before CPE were observed, LFnTcdB¹⁻⁵⁰⁰ plus PA was added to cells and was added every 30 minutes thereafter up to 7 h. Cells were observed and CPE, as determined by cell rounding, were recorded at each of the indicated time points.

In vitro Inhibition of TcdB

If LFnTcdB¹⁻⁵⁰⁰ inhibits the activity of TcdB by interacting with substrate, then inhibition should be observed in an in vitro assay. Glucosylation assays using HeLa extracts as substrate were performed in the presence of LFnTcdB¹⁻⁵⁰⁰ or an equivalent amount of buffer. This assay was performed in triplicate and in vitro glucosylation was reduced by 25.4% +/- 6.25 in assays with inhibitor present compared to assays with no inhibitor added (Figure 23).

In vitro glucosylation of substrates prepared from cells treated with TcdB and inhibitor

Glucosylation assays were performed on extracts prepared from cells treated with TcdB or cotreated with TcdB and LFnTcdB¹⁻⁵⁰⁰. If substrate was protected in cells where inhibitor was present, then it should be accessible to TcdB in the subsequent in vitro assay. Interestingly, a target was found that was protected from modification in cells treated with the toxin and inhibitor, but not TcdB alone (Figure 24). This target was larger than the predicted size for Rho, Rac, and Cdc42. The target may be a yet unidentified substrate of TcdB, or it may be an SDS-resistant protein complex containing Rho, Rac, or Cdc42.

Time-course of inhibition

LFnTcdB¹⁻⁵⁰⁰ and PA were added to cells either prior to or subsequent to TcdB treatment. Cells were amended with fresh inhibitor at 1 h intervals following addition of TcdB (for

1 2

Figure 23. In vitro competition. Glucosylation assays were performed with TcdB (Lane 1) or TcdB in the presence of LFnTcdB1-500 (Lane 2). The reactions were incubated for 25 minutes and the gels were exposed to film for 5 days. This is a representative sample of triplicate assays.

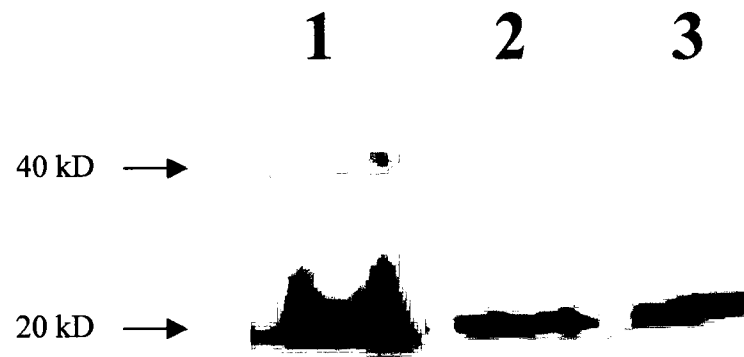


Figure 24. Differential Glucosylation of Extracts Prepared from Cells Treated With TcdB or TcdB plus Inhibitor. Hela cell extracts were prepared from treated cells and tested for glucosylation in vitro. 1, untreated; 2, TcdB treated; 3, TcdB, LFnTcdB¹⁻⁵⁰⁰ and PA treated. All extracts were treated with TcdB in vitro. A target of about 40kD was glucosylated in extracts from untreated cells or in extracts prepared from cells treated with TcdB and inhibitor but not in extracts prepared from TcdB treated cells.

cells pretreated with inhibitor) or 1 h intervals following inhibitor addition (for post-treatment with inhibitor). Cells were amended with inhibitor for 8 hours at which time CPE were determined. We found that this inhibitor was able to block the effects of TcdB on cells when added as much as 40 minutes before toxin treatment or up to 40 minutes following TcdB treatment (Figure 25).

Construction, Purification and Analysis of Amino-terminal Deletions and site-Directed Mutants of the TcdB Enzymatic Domain Fused to LFn

In order to further characterize the TcdB enzymatic domain, and determine the minimal region required for glucosylation activity, amino terminal deletions were constructed. Fragments containing small deletions at the amino-terminal end of the enzymatic domain of TcdB have not been previously characterized. Cloning PCR products into the BamHI/XhoI site of pABII generated the fusions LFnTcdB³⁵⁻⁵⁵⁶ and LFnTcdB⁶⁷⁻⁵⁵⁶. These fusions were tested for glucosylation activity, and it was determined that deleting as little as 35 residues from the amino terminal end of the TcdB glucosylation domain abolished enzymatic activity. This was determined to be due to a loss of glucosylhydrolase activity (Table 5).

Three site-directed mutants were generated in order to further characterize the TcdB enzymatic domain. Deletions of the enzymatic domain most certainly result in conformational changes. These changes cannot be identified using protease digestion since truncated proteins will result in different digestion patterns regardless of conformation. The TcdB enzymatic domain contains a single cysteine residue at position

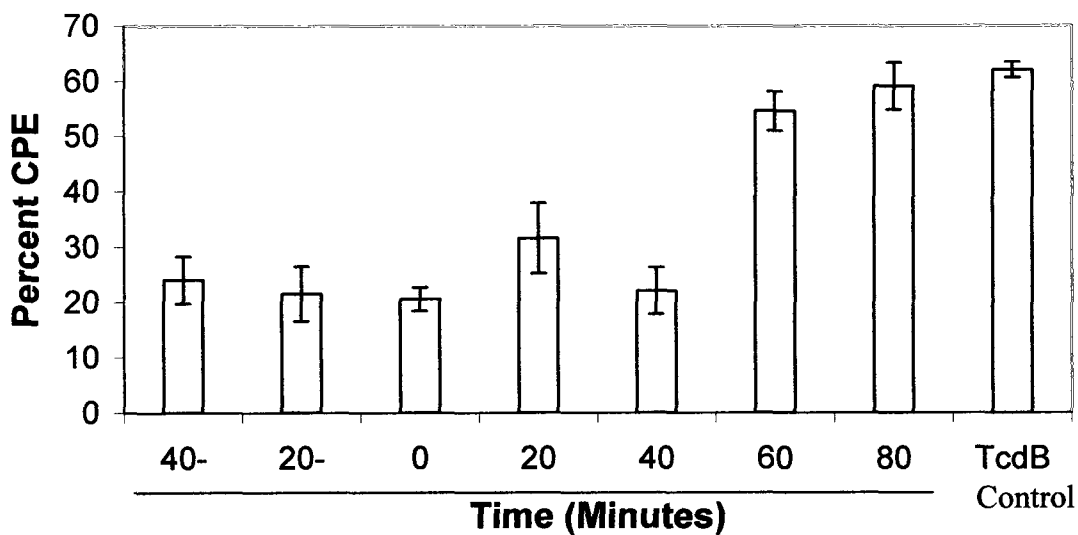


Figure 25. Inhibition of TcdB cytopathic effects prior to or following TcdB treatment. HeLa cells (3×10^4) were plated in a 96 well plate and allowed to adhere overnight. The following day cells were treated with LFnTcdB¹⁻⁵⁰⁰ at the indicated time-points, either prior to or following TcdB treatment. Cells were amended with inhibitor every hour following the initial treatment and CPE were scored (as determined by cell rounding) after 8 hours. Each value is an average of two independent samples and error bars mark the standard deviation from the mean.

Table 5. Glucosylhydrolase Activity of LFnTcdB Amino-Terminal Deletion Mutants. Hydrolase Activity is Expressed as a Percentage of Total UDP-Glucose Present In the Reaction. 9 pmol of each fusion or 3 pmol of TcdB were added to the indicated reaction. Values represent an average of duplicate assays.

Toxin/Fusion	% Hydrolysis	+/-
TcdB	24.6	1.22
LFnTcdB35-556	0	0.11
LFnTcdB67-556	0	0.24

365 in the putative substrate recognition region. Pilot studies using N-ethylmaleimide indicated that cells could be protected from CPE by modification of this residue. To test whether or not we may be able to interfere with substrate recognition by modifying this residue, conservative (C365S) or non-conservative (C365W) mutations of cysteine 365 were constructed using a site-directed mutagenesis kit. One previously characterized mutant W102A, found to be defective in UDP-glucose binding [51], was constructed in a similar fashion. These site-directed mutant fusion proteins were tested for glucosylhydrolase activity, glucosylation activity and CPE on HeLa cells. It was determined that only the C365S mutant retained glucosylation and cytotoxic activity comparable to LFnTcdB¹⁻⁵⁵⁶ (Figure 26).

Hydrolase Activity of Site-directed Mutants of the TcdB Enzymatic Domain

Each of the site-directed mutants was tested for the ability to hydrolyze [¹⁴C] UDP-glucose. It was determined that each of the proteins that were inactive for glucosylation was also void of glucosylhydrolase activity (Table 6).

V8 Protease Digestion

In order to determine if conformational changes might be responsible for the loss of hydrolase activity in the site-directed mutants, LFnTcdB¹⁻⁵⁵⁶, LFnTcdB^{C365W}, and LFnTcdB^{W102A} were digested with V8 protease and the digestion profiles were compared by immunoblot using an antibody to the amino-terminal His-tag. The digestion patterns

A.

1 2 3 4

RhoA

Rac

Cdc42

B.

Fusion (ng)	LFnTcdB1-556	LFnTcdBC365S	LFnTcdBC365W	LFnTcdBW102A
150	90%	88%	13%	12%
15	50.50%	46%	15%	15%
1.5	12.50%	14%	14.50%	13%

Figure 26. Glucosylation and CPE of LFnTcdB Site-Directed Mutants. **A.** Glucosylation assays were performed using recombinant RhoA, Rac1, and Cdc42 as substrate. Lane 1, LFnTcdB^{W102A}; Lane 2, LFnTcdB^{C365W}; Lane 3, LFnTcdB^{C365S}; Lane 4, LFnTcdB¹⁻⁵⁵⁶. **B.** CPE were determined using HeLa cells plated in 96 well plates (3×10^4 cells/well) using a fixed amount of PA (700 ng) and the indicated amount of each fusion. CPE were determined after 90 minutes. Values are an average of duplicate assays.

Table 6. UDP-Glucose Hydrolysis of LFnTcdB Site Directed Mutants. Three pmol of TcdB or 9 pmol of each fusion were added to the indicated reactions. Hydrolysis is expressed as a percent of total UDP-glucose present before separation on an anion exchange column that specifically binds UDP-glucose.

TcdB/Mutant	% Hydrolysis	+/-
TcdB	25.3	0.87
LFnTcdB ^{C365S}	6.2	3.10
LFnTcdB ^{C365W}	1.23	0.51
LFnTcdB ^{W102A}	1.02	0.1

indicate that large conformational changes had not occurred as a result of the substitutions (Figure 27).

Differential Glucosylation

A total of 8 mutants of the enzymatic domain of TcdB were generated (summarized in Figure 28) and characterized for in vitro activity and CPE on tissue culture cells. In vitro protein assays often fail to mimic intracellular conditions and may not accurately reflect the activity of proteins inside cells. In order to determine if these fusions retained glucosylation activity in vivo, each of the fusions were used to treat HeLa cells. After prolonged incubation (16 h) with the indicated fusion, extracts were prepared and used as substrate for glucosylation assays with native TcdB. TcdB was still able to target substrate in extracts prepared from glucosylation defective mutants, but was reduced in the ability to glucosylate targets previously treated with glucosylation active fragments. RhoA (22kD), slightly larger than Rac or Cdc42 (20kD), was not as effectively modified in tissue culture and was still partially accessible in the subsequent in vitro assay (Figure 29).

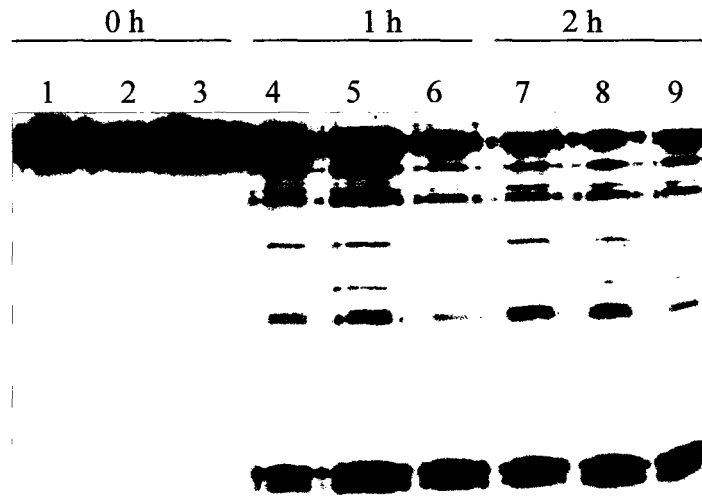


Figure 27. V8 Protease Digestions. Proteins were digested for 0, 1 or 2 hours as indicated. 1, LFnTcdB^{C365W}; 2, LFnTcdB¹⁻⁵⁵⁶; 3, LFnTcdB^{W102A}; 4, LFnTcdB^{C365W}; 5, LFnTcdB¹⁻⁵⁵⁶; 6, LFnTcdB^{W102A}; 7, LFnTcdB^{C365W}; 8, LFnTcdB¹⁻⁵⁵⁶; 9, LFnTcdB^{W102A}. Proteins were analyzed by SDS-PAGE and immunoblotting with anti-His antibody.

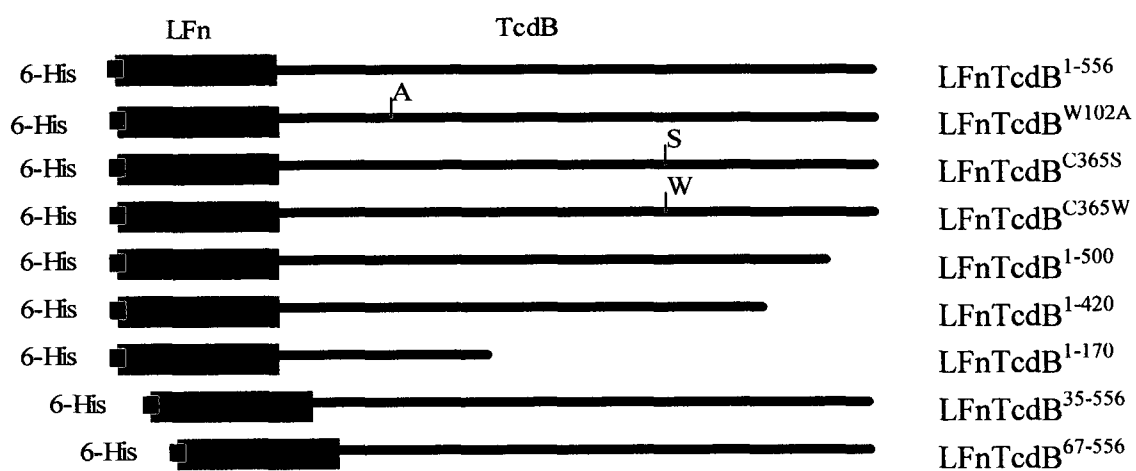


Figure 28. Summary of LFnTcdB Deletion and Site-Directed Mutants.

Toxin B
W102A
C365W
C365S
1-556
1-500
1-420
1-170
33-556
66-556

Figure 29. Differential glycosylation. HeLa cells were treated with each of the indicated fusion proteins and PA for 16 hours. Extracts were then prepared and tested for in vitro glycosylation by native TcdB.

In Vivo Inhibition of TcdB

Since several of the amino-terminal deletion mutants and site-directed mutants were void of glucosylation and glucosylhydrolase activity, they were tested for the ability to inhibit CPE of TcdB in tissue culture cells. Cells were cotreated with TcdB and each of the LFnTcdB mutant proteins plus PA. From Figure 30 it is obvious that each of these inhibitors, the amino-terminal deletions, and the site-directed mutants with substitutions in the cosubstrate-binding region, or the putative substrate recognition region inhibited toxicity by TcdB.

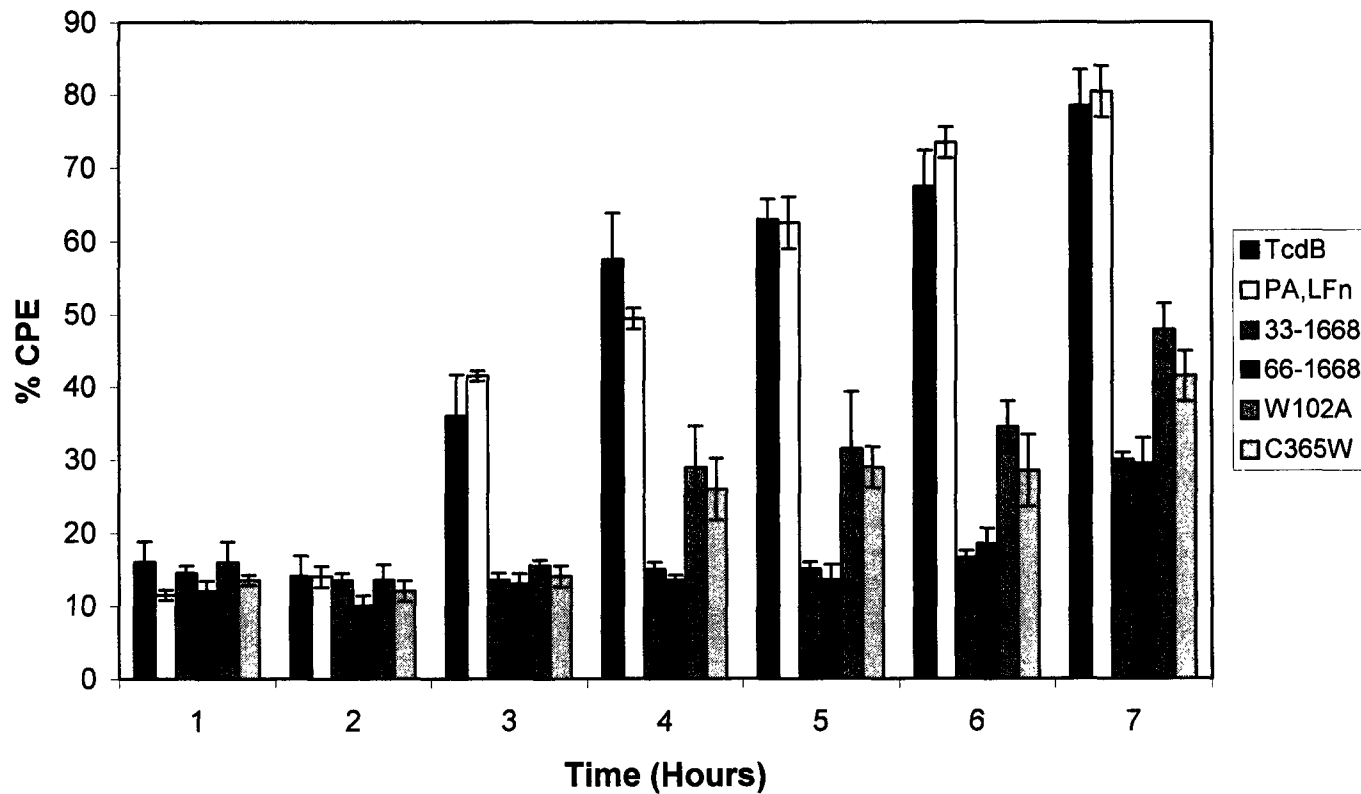


Figure 30. Inhibitory Capacity of LFnTcdB Amino-Terminal and Site-Directed Mutants. HeLa cells were plated in 96 well plates and were treated with PA plus the indicated fusion protein and TcdB. CPE were recorded for each condition at 1 h intervals for 7 h. Each sample was performed in triplicate and error bars mark the standard deviation from the mean.

DISCUSSION

Five LCTs are produced by three different species of clostridia and all are relevant to disease in both humans and animals. *C. difficile* is responsible for CDAD, while *C. novyi* and *C. sordellii* have been implicated in gas gangrene infections. The toxins produced by these organisms are largely responsible for the diseases they cause.

The glucosylation activity of TcdB has not previously been directly linked to death of an animal. Curiously, TcdA, which encodes a similar enzymatic activity but is 1000-fold less cytotoxic than TcdB, has a similar lethal dose [52]. Additionally, TcdA and TcdB are unusually large toxins of which, the majority of residues are completely uncharacterized, thus introducing the possibility that other enzymatic activities that contribute to death are encoded in the full-length toxins. Taking advantage of the PA-LFn delivery system, we were able to demonstrate, for the first time, that the glucosylation domain of TcdB is sufficient to cause death in an animal model.

Although all LCTs share a similar enzymatic activity, they vary in their ability to cause cytopathic effects on cells. TcdB is more cytotoxic than TcdA or TcsL and has been reported to have a 1000 fold greater enzymatic activity than TcdA when tested on substrates RhoA, Rac1, and Cdc42. Interestingly, TcdB and TcsL have been reported to have a similar hydrolase activity and an equal ability to modify the substrate Rac,

suggesting the greater toxicity of TcdB compared to TcsL is due to the slower cell entry of TcsL rather than reduced enzymatic activity [53]. The results we obtained using lysosomotropic agents to follow the cellular entry of TcdB and TcsL confirmed that TcsL does enter HeLa cells more slowly than TcdB thus accounting for the slower CPE of TcsL.

This work has demonstrated the effectiveness of using PA, LFn to deliver fragments of LCTs to the cytosol of cells. Deletion, site-directed mutants and domain swapping experiments have begun to map regions of these toxins important for substrate recognition as well as hydrolase and transferase activities [12, 37, 51]. Until now these experiments were very cumbersome and required microinjecting large amounts of the mutant proteins into mammalian cells. The LFnTcdB fusions described herein will serve as a model for construction of LFn fusions of the enzymatic domains of other LCTs. These tools will prove invaluable for structure function studies of LCTs as has already been demonstrated herein using the enzymatic domain of TcdB.

Another advantage of using the PA-LFn system to characterize LCTs, is the ability to identify the effects of mutant forms of these toxins within cells. The mutant forms of the TcdB enzymatic domain have been useful for detecting *in vivo* inhibition and for determining the effects of this inhibitor within cells (ie. preventing modification of targets). Additionally, the inhibitor provided a unique tool for dissecting the events occurring following membrane translocation. While lysosomotropic inhibitors have proved useful for following cell entry by bacterial toxins, tools to analyze events

following translocation have not been previously reported. Since these inhibitors were shown to block toxin activity within the cytosol, this provided an opportunity to analyze an intracellular toxin after membrane translocation. Our data show that addition of inhibitor at 40 minutes after TcdB treatment is still able to protect cells from CPE (Figure 26). Taking into account the 20 minutes that it takes anthrax toxin to enter the cytosol, we can conclude that CPE can be blocked in the cytosol for up to 60 min after extracellular toxin treatment. Furthermore, results from bafilomycin A1 experiments indicate that TcdB enters the cytosol 40-50 min after toxin treatment (Figure 8). Taken together, these data indicate that irreversible CPE can be blocked within 20 minutes following cytosolic entry of TcdB.

One possible drawback of fusing LFn to fragments of TcdB is the possibility of disrupting folding of these fragments and thus attenuating otherwise normal enzymatic activity. The results that I have obtained using LFnTcdB fusion proteins corresponds very well with results of other groups who have microinjected similar fragments of TcdB. For example, Hoffman et al. generated deletions of TcdB and found that an amino-terminal 546 amino acid fragment of TcdB contained enzymatic activity, while a 516 amino acid fragment was 1000 fold less active [36]. This corresponds very well to the activity that I observed with the LFnTcdB¹⁻⁵⁵⁶ (active) and LFnTcdB¹⁻⁵⁰⁰ (inactive) fusion proteins. Additionally, the site-directed mutant W102A was first constructed and characterized by Busch et al. and found to possess a 1000 fold reduction in enzymatic activity compared to the wild type fragment [51], similar to the results I obtained by generating the same mutation in LFnTcdB¹⁻⁵⁵⁶.

This work has contributed to the basic understanding of the structure of LCTs in general. Mutational analyses of LCTs, taken as a whole, provide insight into the structure of the enzymatic region of these toxins. Deletions as small as 35 amino acids from either the amino-terminal (Table 5) or carboxy-terminal ends [36] of the enzymatic domain render the protein inactive. This inactivation is due to a loss of hydrolase activity although neither of these regions has been shown to directly be involved in hydrolase activity, and neither shows homology with other known glucosyltransferases. Most likely, hydrolase activity is sensitive to small changes in conformation and these regions serve to stabilize the protein. The LFnTcdB¹⁻⁵⁵⁶ fusion protein is reduced in glucosylhydrolase activity by approximately 12 fold and cytotoxicity by 100 fold compared to native TcdB. This is probably due to the addition of LFn (255 residues) to the amino-terminus of TcdB¹⁻⁵⁵⁶ since other groups have reported enzymatic activity that paralleled that of the wild-type toxin from similar deletions of TcdB [36]. It is important, however, to use caution when making a direct comparison between the activities of LFnTcdB¹⁻⁵⁵⁶ and the full-length toxin since they were purified by different methods and both proteins show reduced activity after storage.

Toxin A (TcdA) and Toxin B (TcdB) are the major virulence factors in the onset of *Clostridium difficile* associated disease (CDAD). *Clostridium difficile* is the most common etiologic agent of hospital-acquired diarrhea accounting for 10-25% of reported cases [54]. This organism is resistant to most commonly used broad range antibiotics including clindamycin, ampicillin, amoxicillin, and cephalosporins. Antibiotic treatment

inhibits normal gut flora while allowing the colonization of resistant *C. difficile* in previously exposed patients. Since only two antibiotics, vancomycin and metronidazole are effective at treating CDAD, which can range from mild diarrhea to the more severe pseudomembranous colitis, antibiotic resistant strains of *C. difficile* are a real concern.

During the analysis of the enzymatic domain of TcdB, we found several mutants of this domain that were capable of ameliorating the CPE of this toxin. Due to the seriousness of CDAD, and the complications of treating this disease with antibiotics, these inhibitors provide a potential treatment. Since these inhibitory regions were fused to LFn, they could be easily delivered to patients in conjunction with PA. Experiments where these fusions were injected into mice indicate that effective delivery of these domains is occurring because mice die after injection with 100 fmol of the enzymatic domain of TcdB.

In addition to providing a potential therapy for CDAD, these inhibitors also block the CPE of TcsL from *C. sordellii* (Figure 21), an organism isolated from gas gangrene infections [55, 56]. Clostridial gas gangrene infections are equally as serious as CDAD. Despite treatment with antibiotics, hyperbaric oxygen treatments, and surgery, 25% of cases still result in mortality [57]. The results reported herein, indicate that LFnTcdB¹⁻⁵⁰⁰ also inhibits the effects of TcsL on cells and could be used for the treatment of *C. sordellii* infections as well.

While this work did not show conclusively that TcdA was inhibited by this mutant form of TcdB, TcdA shares substrates with TcdB and TcsL and LFnTcdB¹⁻⁵⁰⁰ has been shown to inhibit CPE of both of these toxins. Additionally, LFnTcdB¹⁻⁵⁰⁰ was able to protect cells from the toxic effects of *C. difficile* supernatants that contain both TcdA and TcdB. Taken together, these results provide strong evidence for the inhibition of TcdA CPE by the LFnTcdB¹⁻⁵⁰⁰ fusion protein.

A major question still exists as to the mechanism of inhibition of LCTs by LFnTcdB¹⁻⁵⁰⁰. The inhibition most likely occurs because of a competition for substrate or cosubstrate, although we could not rule out the possibility that LCTs form a higher order complex, and that these mutant forms somehow interfered with the assembly of this complex. Our results indicate that the competition is occurring inside of the cell since LFnTcdB¹⁻⁵⁰⁰ is capable of inhibiting CPE of TcdB¹⁻⁵⁵⁶ expressed inside transfected CHO cells. Additionally, the inhibition does not seem to be due to LFnTcdB¹⁻⁵⁰⁰ sequestering UDP-glucose in the cell because a previously described site-directed mutant defective in UDP-glucose binding -demonstrating a K_m that is 200 fold less than the wild type fragment [51]- was also able to inhibit CPE when generated as an LFn fusion and delivered to cells in conjunction with PA.

TcsL and TcdB have been shown to interact with amino acids 22-27 of their target GTPases. These amino acids are part of the p-loop and $\alpha 1$ helix both of which are known to interact with GEFs, GAPs, and/or downstream effector proteins [58]. If inhibition was occurring through protein interaction with substrate, then physiological effects on cells

may be observed in the absence of enzymatic activity. For example, LFnTcdB¹⁻⁵⁰⁰ lacks enzymatic activity, but if it still interacts with substrate, it could prevent signaling to downstream effector proteins. A change in cell morphology was observed after extended treatment with the inhibitor suggesting there may be an interaction with substrate.

If inhibition was due to interaction of the inhibitor with substrate thus reducing the amount of substrate accessible to toxin, then inhibition should also be observed in vitro which was consistent with our results (Figure 24). In order to confirm substrate was protected from TcdB modification inside the cell in the presence of inhibitor, differential glucosylation assays were carried out on HeLa extracts prepared from cells during inhibition experiments. A target was identified, which was protected in cells treated with inhibitor and toxin, but not in cells treated with toxin alone (Figure 25). Interestingly, this target was much larger than Rho, Rac, or Cdc42. While one explanation seems to be that this target is a complex containing Rho, Rac, or Cdc42, it may be a target of LCTs that has not previously been identified. A likely candidate is one of the heteromeric G proteins, which contain some sequence similarity to small Rho GTPases.

Inhibition of TcsL CPE by the attenuated enzymatic domain of TcdB raises obvious questions. If TcsL targets different substrates than TcdB and inhibition is due to blocking substrate interaction, then why was TcsL inhibited by the substrate interacting region of TcdB? Since TcsL has recently been shown to modify the TcdB substrates Rho, Rac, and Cdc42 [12], it may be that inhibiting glucosylation of these substrates is sufficient to rescue cells from TcsL CPE. Alternatively, efficient targeting of Ras, Rap, and Ral may

require at least two substrate recognition sites on the toxin. The second possibility is supported by results obtained from chimeric fusion proteins of TcdB and TcsL, where region 364-468 of TcdB and TcsL were sufficient for targeting Rho, Rac and Cdc42, but TcsL required this region and region 468-516 to efficiently target Ras, Rap, and Ral [12]. I propose that the truncated fusion proteins are able to bind to TcsL and TcdB target GTPases thus blocking interaction of the native toxins. I have generated a model, which fits the current understanding of TcdB and TcsL substrate interacting regions, to explain how this interaction may occur (Figure 31).

LFnTcdB fusion proteins provide insight into the location of the substrate recognition region of LCTs. The substrate recognition region of TcdB was previously narrowed to a region encompassing amino acids 364-468 [12]. Smaller regions have not been tested for the ability to interact with Rho, Rac, and Cdc42. Generation of a mutation at position 365 previously believed to be part of the substrate recognition region, was sufficient to disrupt hydrolase activity, but did not impair substrate binding determined by this fragments ability to compete with wild type TcdB. These results indicate this region is probably not involved in substrate recognition. Furthermore, the effectiveness of the 1-420 amino acid fusion protein at inhibiting the activity of TcdB indicates that LFnTcdB¹⁻⁴²⁰ contains an essential substrate recognition region. Taken together, these results indicate that the substrate recognition region of TcdB lies between amino acids 366-420.

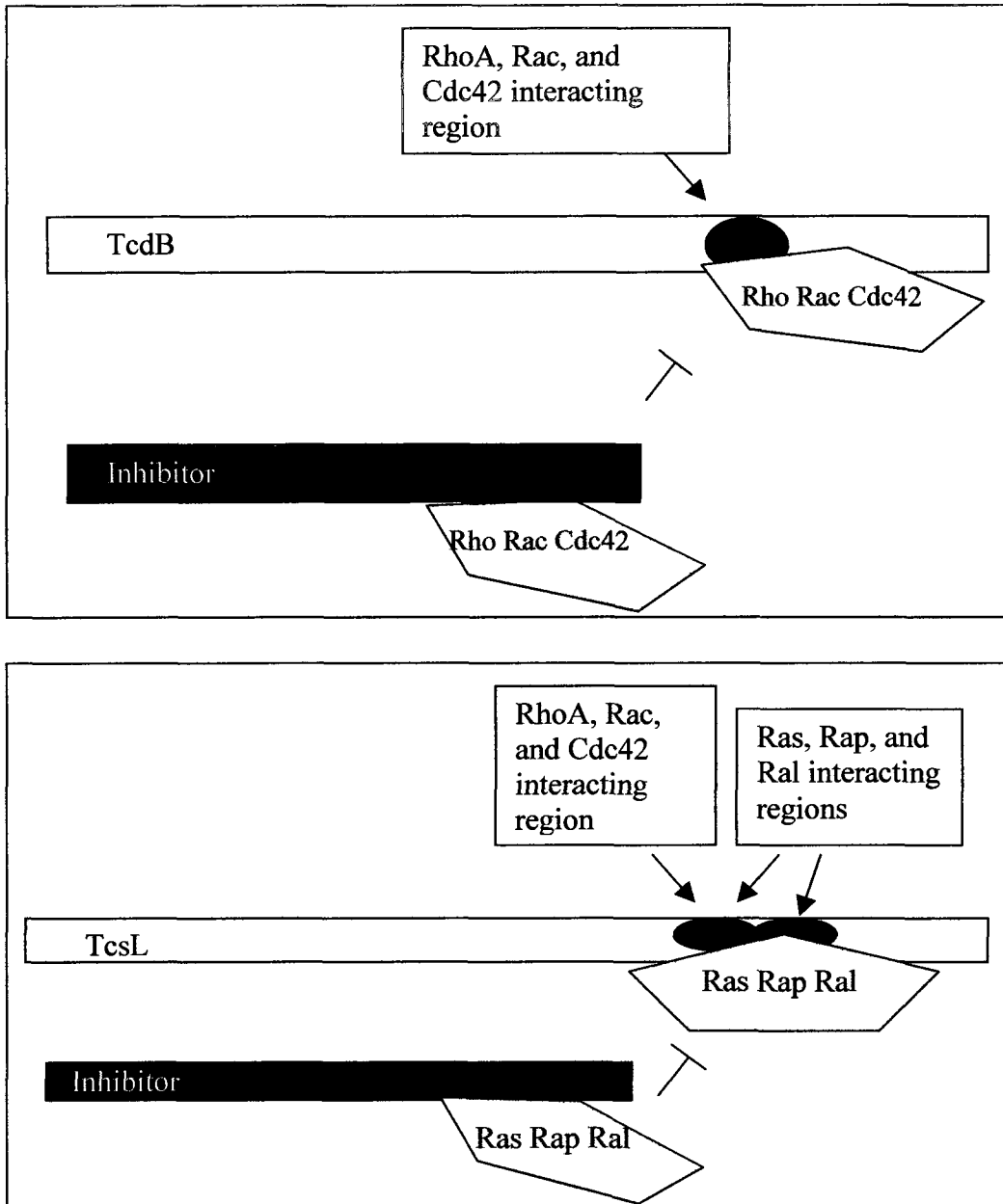


Figure 31. Model For Inhibition of LCTs by the Inhibitor LFnTcdB¹⁻⁵⁰⁰. Rho, Rac, and Cdc42 have one substrate interacting region, and substrates interact with inhibitor reducing the interaction of TcdB with substrate. Ras Rap and Ral targeting requires two separate or overlapping substrate interacting regions, one which is shared with Rho, Rac, and Cdc42. The second is unique to Ras, Rap, and Ral. Interaction of LFnTcdB¹⁻⁵⁰⁰ with Ras Rap and Ral through the first shared recognition site is sufficient to inhibit the interaction of these substrates with TcsL.

PA/LFn has proved vital for the cytosolic delivery of the truncated forms of TcdB described in this research. The LFnTcdB fusion proteins provide the first examples of truncated virulence factors that are able to inhibit the native virulence factor inside a mammalian cell. This inhibition activity has allowed us to narrow the substrate-binding region of TcdB. In addition, by cotreating cells with PA/LFnTcdB¹⁻⁵⁰⁰ and TcdB we discovered a novel TcdB cellular target, which was protected from glucosylation in extracts from TcdB/inhibitor treated cells but not in extracts from TcdB treated cells. There are at least two lines of research that would be interesting to pursue in future work. Generating LFnTcdB fusion proteins with deletions in this substrate-binding region (amino acids 366-420) could further narrow the substrate recognition region of this toxin. Secondly, identification of this novel TcdB cellular target will provide insight into the cellular intoxication process for TcdB and LCTs in general.

BIBLIOGRAPHY

1. Falnes, P.O. and K. Sandvig, *Penetration of protein toxins into cells*. Curr Opin Cell Biol, 2000. **12**(4): p. 407-13.
2. Mylonakis, E., E.T. Ryan, and S.B. Calderwood, *Clostridium difficile--Associated diarrhea: A review*. Arch Intern Med, 2001. **161**(4): p. 525-33.
3. Barbut, F., et al., *Epidemiology of recurrences or reinfections of Clostridium difficile-associated diarrhea*. J Clin Microbiol, 2000. **38**(6): p. 2386-8.
4. Tacconelli, E., et al., *Clostridium difficile-associated diarrhea in human immunodeficiency virus infection--a changing scenario [letter; comment]*. Clin Infect Dis, 1999. **28**(4): p. 936-7.
5. Aktories, K., *Bacterial toxins that target Rho proteins*. J Clin Invest, 1997. **99**(5): p. 827-9.
6. Ball, D.W., et al., *Purification and characterization of alpha-toxin produced by Clostridium novyi type A*. Infect Immun, 1993. **61**(7): p. 2912-8.
7. Boquet, P., et al., *Toxins from anaerobic bacteria: specificity and molecular mechanisms of action*. Curr Opin Microbiol, 1998. **1**(1): p. 66-74.
8. Feltis, B.A., et al., *Clostridium difficile toxins A and B can alter epithelial permeability and promote bacterial paracellular migration through HT-29 enterocytes. [In Process Citation]*. Shock, 2000. **14**(6): p. 629-34.
9. Garrett, W.S., et al., *Developmental control of endocytosis in dendritic cells by Cdc42*. Cell, 2000. **102**(3): p. 325-34.
10. Nusrat, A., et al., *Clostridium difficile toxins disrupt epithelial barrier function by altering membrane microdomain localization of tight junction proteins*. Infect Immun, 2001. **69**(3): p. 1329-36.
11. Popoff, M.R., et al., *Ras, Rap, and Rac small GTP-binding proteins are targets for Clostridium sordellii lethal toxin glucosylation*. J Biol Chem, 1996. **271**(17): p. 10217-24.
12. Hofmann, F., C. Busch, and K. Aktories, *Chimeric clostridial cytotoxins: identification of the N-terminal region involved in protein substrate recognition*. Infect Immun, 1998. **66**(3): p. 1076-81.
13. Parada, L.F., et al., *Human EJ bladder carcinoma oncogene is homologue of Harvey sarcoma virus ras gene*. Nature, 1982. **297**(5866): p. 474-8.
14. Mackay, D.J. and A. Hall, *Rho GTPases*. J Biol Chem, 1998. **273**(33): p. 20685-8.
15. Kjoller, L. and A. Hall, *Signaling to Rho GTPases*. Exp Cell Res, 1999. **253**(1): p. 166-79.

16. Bos, J.L., *ras oncogenes in human cancer: a review*. *Cancer Res*, 1989. **49**(17): p. 4682-9.
17. Clark, W.R., et al., *Molecular pathways of CTL-mediated cytotoxicity*. *Immunological Reviews*, 1995. **146**: p. 33-44.
18. Sander, E.E. and J.G. Collard, *Rho-like GTPases: their role in epithelial cell-cell adhesion and invasion*. *Eur J Cancer*, 1999. **35**(14): p. 1905-11.
19. Aepfelbacher, M., et al., *Bacterial toxins block endothelial wound repair. Evidence that Rho GTPases control cytoskeletal rearrangements in migrating endothelial cells*. *Arterioscler Thromb Vasc Biol*, 1997. **17**(9): p. 1623-9.
20. Benard, V., G.M. Bokoch, and B.A. Diebold, *Potential drug targets: small GTPases that regulate leukocyte function*. *Trends Pharmacol Sci*, 1999. **20**(9): p. 365-70.
21. Doussau, F., et al., *A Rho-related GTPase is involved in Ca(2+)-dependent neurotransmitter exocytosis*. *J Biol Chem*, 2000. **275**(11): p. 7764-70.
22. Orrico, A., et al., *A mutation in the pleckstrin homology (PH) domain of the FGD1 gene in an Italian family with faciogenital dysplasia (Aarskog-Scott syndrome)*. *FEBS Lett*, 2000. **478**(3): p. 216-20.
23. Kim, A.S., et al., *Autoinhibition and activation mechanisms of the Wiskott-Aldrich syndrome protein*. *Nature*, 2000. **404**(6774): p. 151-8.
24. Clerk, A. and P.H. Sugden, *Small guanine nucleotide-binding proteins and myocardial hypertrophy*. *Circ Res*, 2000. **86**(10): p. 1019-23.
25. Just, I., et al., *Glucosylation of Rho proteins by Clostridium difficile toxin B*. *Nature*, 1995. **375**(6531): p. 500-3.
26. Ihara, K., et al., *Crystal structure of human RhoA in a dominantly active form complexed with a GTP analogue*. *J Biol Chem*, 1998. **273**(16): p. 9656-66.
27. Borrow, P., et al., *Antiviral pressure exerted by HIV-1-specific cytotoxic T lymphocytes (CTLs) during primary infection demonstrated by rapid selection of CTL escape virus [see comments]*. *Nature Medicine*, 1997. **3**(2): p. 205-11.
28. Freeman, J.L., A. Abo, and J.D. Lambeth, *Rac "insert region" is a novel effector region that is implicated in the activation of NADPH oxidase, but not PAK65*. *J Biol Chem*, 1996. **271**(33): p. 19794-801.
29. Zhou, K., et al., *Guanine nucleotide exchange factors regulate specificity of downstream signaling from Rac and Cdc42*. *J Biol Chem*, 1998. **273**(27): p. 16782-6.
30. Bishop, A.L. and A. Hall, *Rho GTPases and their effector proteins*. *Biochem J*, 2000. **348 Pt 2**: p. 241-55.
31. Coso, O.A., et al., *The small GTP-binding proteins Rac1 and Cdc42 regulate the activity of the JNK/SAPK signaling pathway*. *Cell*, 1995. **81**(7): p. 1137-46.
32. Minden, A., et al., *Selective activation of the JNK signaling cascade and c-Jun transcriptional activity by the small GTPases Rac and Cdc42Hs*. *Cell*, 1995. **81**(7): p. 1147-57.
33. Hill, C.S., J. Wynne, and R. Treisman, *The Rho family GTPases RhoA, Rac1, and CDC42Hs regulate transcriptional activation by SRF*. *Cell*, 1995. **81**(7): p. 1159-70.

34. Boquet, P., *Bacterial toxins inhibiting or activating small GTP-binding proteins*. Ann N Y Acad Sci, 1999. **886**: p. 83-90.
35. Boquet, P., P.J. Sansonetti, and G. Tran Van Nhieu, *Rho GTP-binding proteins as targets for microbial pathogens*. Prog Mol Subcell Biol, 1999. **22**: p. 183-99.
36. Hofmann, F., et al., *Localization of the glucosyltransferase activity of Clostridium difficile toxin B to the N-terminal part of the holotoxin*. J Biol Chem, 1997. **272**(17): p. 11074-8.
37. Busch, C., et al., *Characterization of the catalytic domain of clostridium novyi alpha- toxin [In Process Citation]*. Infect Immun, 2000. **68**(11): p. 6378-83.
38. Wagenknecht-Wiesner, A., et al., *Delineation of the catalytic domain of Clostridium difficile toxin B- 10463 to an enzymatically active N-terminal 467 amino acid fragment*. FEMS Microbiol Lett, 1997. **152**(1): p. 109-16.
39. Busch, C., et al., *A common motif of eukaryotic glycosyltransferases is essential for the enzyme activity of large clostridial cytotoxins*. J Biol Chem, 1998. **273**(31): p. 19566-72.
40. Arora, N. and S.H. Leppla, *Residues 1-254 of anthrax toxin lethal factor are sufficient to cause cellular uptake of fused polypeptides*. Journal of Biological Chemistry, 1993. **268**(5): p. 3334-41.
41. Milne, J.C., et al., *Protective antigen-binding domain of anthrax lethal factor mediates translocation of a heterologous protein fused to its amino- or carboxy-terminus*. Molecular Microbiology, 1995. **15**(4): p. 661-6.
42. Arora, N. and S.H. Leppla, *Fusions of anthrax toxin lethal factor with shiga toxin and diphtheria toxin enzymatic domains are toxic to mammalian cells*. Infection & Immunity, 1994. **62**(11): p. 4955-61.
43. Ballard, J.D., R.J. Collier, and M.N. Starnbach, *Anthrax toxin-mediated delivery of a cytotoxic T-cell epitope in vivo*. Proceedings of the National Academy of Sciences of the United States of America, 1996. **93**(22): p. 12531-4.
44. Ballard, J.D., R.J. Collier, and M.N. Starnbach, *Anthrax Toxin as a Molecular Tool for Stimulation of Cytotoxic T Lymphocytes: Disulfide-Linked Epitopes, Multiple Injections, and Role of CD4⁺ Cells*. Infection and Immunity, 1998. **66**(10): p. 4696-4699.
45. Spyres, L.M., et al., *Cytosolic delivery and characterization of the TcdB glucosylating domain by using a heterologous protein fusion*. Infect Immun, 2001. **69**(1): p. 599-601.
46. Starnbach, M.N., M.J. Bevan, and M.F. Lampe, *Protective cytotoxic T lymphocytes are induced during murine infection with Chlamydia trachomatis*. Journal of Immunology, 1994. **153**(11): p. 5183-9.
47. Ciesla, W.P., Jr. and D.A. Bobak, *Clostridium difficile toxins A and B are cation-dependent UDP-glucose hydrolases with differing catalytic activities*. J Biol Chem, 1998. **273**(26): p. 16021-6.
48. Qa'Dan, M., L.M. Spyres, and J.D. Ballard, *pH-Enhanced Cytopathic Effects of Clostridium sordellii Lethal Toxin*. Infect Immun, 2001. **69**(9): p. 5487-93.
49. Kane, J.F., *Effects of rare codon clusters on high-level expression of heterologous proteins in Escherichia coli*. Curr Opin Biotechnol, 1995. **6**(5): p. 494-500.

50. Bonekamp, F., et al., *Codon-defined ribosomal pausing in Escherichia coli detected by using the pyrE attenuator to probe the coupling between transcription and translation*. Nucleic Acids Res, 1985. **13**(11): p. 4113-23.
51. Busch, C., et al., *Involvement of a conserved tryptophan residue in the UDP-glucose binding of large clostridial cytotoxin glycosyltransferases*. J Biol Chem, 2000. **275**(18): p. 13228-34.
52. von Eichel-Streiber, C., et al., *Purification of two high molecular weight toxins of Clostridium difficile which are antigenically related*. Microb Pathog, 1987. **2**(5): p. 307-18.
53. Chaves-Olarte, E., et al., *Toxins A and B from Clostridium difficile differ with respect to enzymatic potencies, cellular substrate specificities, and surface binding to cultured cells*. J Clin Invest, 1997. **100**(7): p. 1734-41.
54. Barbut, F. and J.C. Petit, *[Epidemiology, risk factors and prevention of Clostridium difficile nosocomial infections]*. Pathol Biol (Paris), 2000. **48**(8): p. 745-55.
55. el Sanousi, S.M. and M.T. Musa, *Note on an association of Clostridium novyi type A and Clostridium sordellii with a case of gas-gangrene in a Zebu cow*. Rev Elev Med Vet Pays Trop, 1989. **42**(3): p. 391-2.
56. Bitti, A., et al., *A fatal postpartum Clostridium sordellii associated toxic shock syndrome*. J Clin Pathol, 1997. **50**(3): p. 259-60.
57. Korhonen, K., *Hyperbaric oxygen therapy in acute necrotizing infections. With a special reference to the effects on tissue gas tensions*. Ann Chir Gynaecol, 2000. **89 Suppl 214**: p. 7-36.
58. Muller, S., C. von Eichel-Streiber, and M. Moos, *Impact of amino acids 22-27 of Rho-subfamily GTPases on glucosylation by the large clostridial cytotoxins TcsL-1522, TcdB-1470 and TcdB-8864*. Eur J Biochem, 1999. **266**(3): p. 1073-80.